Authors' draft manuscript, peer-reviewed

Could be different from the final variant after pre-publication editing

Published online February 12, 2018 in Journal of Cell Biology,

http://jcb.rupress.org/content/early/2018/02/09/jcb.201707027 , DOI: 10.1083/jcb.201707027

SLAMF1 is required for TLR4-mediated TRAM-TRIF dependent signaling in human macrophages

Maria Yurchenko[1,3,*], Astrid Skjesol[1], Liv Ryan[1], Gabriel Mary Richard[1], Richard Kumaran Kandasamy[1], Ninghai Wang[2], Cox Terhorst[2], Harald Husebye[1,3, †], Terje Espevik[1,3, †]

[1]Centre of Molecular Inflammation Research, Norwegian University of Science and Technology, Trondheim, Norway

[2]Division of Immunology, Beth Israel Deaconess Medical Center, Harvard Medical School, Boston, MA 02215, USA

[3]The Central Norway Regional Health Authority, Trondheim, Norway

[†]Equal contribution

***Corresponding author:**

E-mail: mariia.yurchenko@ntnu.no

ORCID ID: orcid.org/0000-0002-0516-4747

Mailing address: CEMIR, PO Box 8905 MTFS, NO-7491 Trondheim, Norway

Condensed title: **SLAMF1 regulates TLR4-TRAM-TRIF-mediated signaling**

Summary

Yurchenko *et al*. discover that the Ig-like receptor molecule SLAMF1 enhances production of type I interferon induced by Gram-negative bacteria through modulation of MyD88 independent TLR4 signaling. This makes SLAMF1 a potential target for controlling inflammatory responses against Gram-negative bacteria.

Abstract

Signaling lymphocytic activation molecule family 1 (SLAMF1) is an Ig-like receptor and a costimulatory molecule that initiates signal transduction networks in a variety of immune cells. Here we report that SLAMF1 is required for Toll-like receptor 4 (TLR4)-mediated induction of interferon β (IFNβ) and for killing of Gram-negative bacteria by human macrophages. We found that SLAMF1 controls trafficking of the Toll-receptor-associated molecule (TRAM) from endocytic recycling compartment (ERC) to *E. coli* phagosomes. In resting macrophages SLAMF1 is localized to ERC, but upon addition of *E. coli* it is trafficked together with TRAM from ERC to *E. coli* phagosomes in a Rab11-dependent manner. We found that endogenous SLAMF1 protein interacted with TRAM, and defined key interaction domains as amino acids 68 to 95 of TRAM, and 15 C-terminal amino acids of SLAMF1. Interestingly, SLAMF1-TRAM interaction was observed for human, but not mouse proteins. Overall our observations suggest that SLAMF1 is a new target for modulation of TLR4-TRAM-TRIF inflammatory signaling in human cells.

Introduction

Toll like receptors (TLRs) are pivotal for the defense against multiple pathogens by recognizing pathogen-associated molecular patterns. TLR4 recognizes lipopolysaccharide (LPS) from Gram-negative bacteria in complex with co-receptors myeloid differentiation factor 2 and CD14, and recruits signaling adapters myeloid differentiation primary response gene 88 (MyD88) and MyD88-adapter-like (Mal). This results in an immediate activation of nuclear factor κB (NF-κB) and production of proinflammatory cytokines. TLR4 is also present on endosomes and phagosomes to which the signaling adapter Toll-receptor-associated molecule (TRAM) is recruited (Husebye et al., 2010; Husebye et al., 2006; Kagan et al., 2008). The mechanism controlling TRAM recruitment remains unclear, but seems to be Rab11 dependent (Husebye et al., 2010; Klein et al., 2015; Troutman et al., 2012a).

TRAM is crucial for subsequent recruitment of TIR-domain-containing adapter-inducing interferon-β (TRIF) and other downstream molecules, leading to IFNβ secretion (Fitzgerald et al., 2003b; Husebye et al., 2010; Oshiumi et al., 2003; Yamamoto et al., 2003). The role of endogenous type I IFNs in host defense against bacterial infections could be either beneficial or detrimental. Type I IFNs make macrophages more sensitive to cell death inducing stimuli that could favor bacterial replication and release (Trinchieri, 2010). At the same time type I IFNs are required for the host resistance to group B streptococci, pneumococci and *E. coli* (Mancuso et al., 2007).

Assembly of TLR4-TRAM-TRIF complex followed by the activation of TANK-Binding Kinase 1 (TBK1) results not only in the induction of type I IFNs, but also required for maintenance of the integrity of pathogen-containing vacuoles, and restriction of bacterial proliferation in the cytosol (Radtke et al., 2007; Thurston et al., 2016). Moreover, TBK1 activates Akt-mTOR-HIF1α signaling axis, which orchestrates metabolic reprogramming to aerobic glycolysis in immune cells (Everts et al., 2014; Krawczyk et al., 2010). Glycolysis provides ATP for driving phagocytosis, pro-inflammatory cytokines production, and nicotinamide adenine dinucleotide phosphate (NADPH) for

the NADPH oxidase 2 (NOX2) enzyme to generate reactive oxygen species (ROS) (Kelly and O'Neill, 2015).

SLAMF1/CD150 is a type I glycoprotein belonging to the SLAM subfamily of the CD2-like family of proteins (Cocks et al., 1995; Sidorenko and Clark, 1993). SLAMF1 acts as a co-receptor that can modulate signaling via the tumor necrosis factor (TNF) family and antigen receptors (Makani et al., 2008; Mikhalap et al., 1999; Rethi et al., 2006; Wang et al., 2004). SLAMF1 is involved in regulation of innate immune responses. *Slamf1*$^{-/-}$ bone marrow derived macrophages (BMDMs) are deficient in bacterial killing as they produce less ROS in response to *E. coli*. Mouse SLAMF1 positively regulates NOX2 activity by forming a complex with beclin-1-Vps34-Vps15-UVRAG (Berger et al., 2010; Ma et al., 2012). Thus, it was essential to explore the contribution of SLAMF1 to TLR4-mediated signaling in human cells. Here we show that in human macrophages SLAMF1 acts as a critical regulator of TLR4-mediated signaling from the phagosome by interacting with TRAM adapter and class I Rab11 family interacting proteins (Rab11 FIPs or FIPs), and recruiting the adapter to the TLR4 signaling complex.

Results

SLAMF1 is expressed in human macrophages and localized to Rab11-positive ERC

Previous studies have suggested that SLAMF1 is found in intracellular compartments of human primary dendritic cells and glioblastoma cells (Avota et al., 2011; Romanets-Korbut et al., 2015). Human peripheral blood monocytes do not express SLAMF1 on the plasma membrane (Farina et al., 2004; Romero et al., 2004). Therefore, we first analyzed the cellular distribution of SLAMF1 in human monocytes, macrophages and THP-1 cells by confocal microscopy. In all the cell types examined the major pool of SLAMF1 was located in a peri-nuclear area negative for the Golgi marker GM130 (Fig. 1 A and B). To further define SLAMF1 localization, monocytes were co-stained with markers for different types of endosomes: recycling - (Rab11a) (Fig. 1 C-E), early - (EEA1) and late endosomes (LAMP1) (Fig. 1 C-E). Rab11a also defines the endocytic recycling compartment (ERC), a condensed peri-nuclear region containing tubular membrane structures that originate from the microtubule organizing center (Yamashiro et al., 1984). TRAM and TLR4 are also present in ERC of human monocytes and macrophages (Husebye et al., 2010; Klein et al., 2015).

A marked co-localization was found between SLAMF1 and Rab11 in ERC of resting cells, with Manders' co-localization coefficient tM = 0.683 ± 0.08 (Fig. 1 C), while there was no co-localization with the other endosomal markers (Fig. 1 D and E). As determined by flow cytometry, only 1% of the monocytes and 4% of macrophages showed surface expression of SLAMF1, whereas 40% of the differentiated THP-1-cells were SLAMF1 positive (Fig. 1 F). LPS stimulation increased the surface expression of SLAMF1 in primary macrophages with more than 50% after 6 h of LPS stimulation, with an increase in the total SLAMF1 protein expression (Fig. 1 G and H; and Fig. S1 A). Moreover, various TLR ligands such as Pam3Cys (TLR1/2), FSL-1 (TLR2/6), R848 (TLR7 and -8) and CL075 (TLR8) increased *SLAMF1* mRNA expression in monocytes and macrophages (Fig. 1 I and J), with *E.coli* being the most potent stimulator (Fig. 1 I). These results indicate that several TLRs control SLAMF1 expression in human cells.

In summary, resting macrophages showed very low SLAMF1 surface level expression and the major cellular pool of SLAMF1 was found to be in the ERC. THP-1 cells had more surface SLAMF1, but the major cellular pool was still located in the ERC. These observations suggest that ERC-located SLAMF1 may have a yet undefined function in macrophages.

SLAMF1 is required for TLR4-mediated IFNβ production, but its expression is not regulated by the IFN α/β receptor

Next, we used small interfering RNAs (siRNA) to target SLAMF1 in THP-1 cells (Fig. 2 A) and human macrophages (Fig. 2 B). We found that SLAMF1 silencing caused consistent reduction in LPS-mediated *IFNβ* mRNA levels (Fig. 2 A and B) and IFNβ secretion (Fig. 2 C and D). In contrast, *TNF* mRNA amounts were only reduced at late time points of LPS stimulation, and secretion was affected only in THP-1 cells (Fig. 2 A-D). SLAMF1 silencing impaired both IL-6 and CXCL10 secretion, but did not affect the secretion of IL-1β and IL-8 in THP-1 cells and human macrophages (Fig. 2 E). The phosphorylation of STAT1 and initiation of transcription of IFN-inducible genes, like *CXCL10* are read-outs of IFNβ binding to the IFN α/β receptor (IFNAR) (Toshchakov et al., 2002). IFNAR-dependent STAT1 phosphorylation (Y701) and *CXCL10* mRNA expression in response to LPS were both significantly decreased in THP-1 cells pre-treated by anti-IFNARα/β chain 2 mAbs (Fig. S1 B and C). However, *SLAMF1* mRNA expression was not altered by blocking IFNAR (Fig. S1 D). Thus, *SLAMF1* mRNA expression was not driven by IFNβ mediated signaling.

Upon stimulation with *E. coli* particles, *SLAMF1* silenced THP-1 cells also showed a consistent reduction in *IFNβ* and *TNF* mRNA (Fig. S2 A). However, SLAMF1 silencing in macrophages had no effect on *IFNβ* or *TNF* mRNA expression in response to poly I:C with or without transfection (RIG-I/MDA5 or TLR3) or to TLR8 ligand CL075 (Fig. S2 B-D).

SLAMF1 regulates TLR4-mediated signaling upstream of TBK1 and IRF3

Phosphorylation of Interferon Regulatory Factor 3 (IRF3) transcription factor is critical for the regulation of early *IFNβ* transcription in macrophages (Sakaguchi et al., 2003). TBK1 acts upstream of IRF3 and phosphorylates IRF3 by itself or together with Inhibitor of nuclear factor kappa-B Kinase subunit epsilon (IKKε) (Fitzgerald et al., 2003a). Macrophages silenced for SLAMF1 showed decreased levels in both LPS-induced TBK1 and IRF3 phosphorylation (Fig. 3, top panels). This was also observed in SLAMF1 silenced THP-1 cells stimulated with LPS or *E. coli* particles (Fig. S3 A and B).

Transcription of *IFNβ* is coordinately regulated by several transcription factor families such as IRFs, NF-κB and ATF-2–c-Jun (Ford and Thanos, 2010). To explore events upstream of ATF-2–c-Jun activation, we analyzed the effect of SLAMF1 silencing on LPS-mediated activation of mitogen activated kinases (MAPKs). SLAMF1 silencing resulted in decreased phosphorylation of MAPK kinase kinase 7 (MAP3K)/TAK1 and downstream MAPKs (p38MAPK and JNK1/2) (Fig. 3; and Fig. S3 A). Both p38MAPK and JNK1/2 positively regulate the transcriptional activity of AP1 (ATF-2-c-jun) (Chang and Karin, 2001), and it is therefore likely that the observed reduction in MAPKs phosphorylation upon SLAMF1 silencing may contribute to decreased AP-1 activity.

The total level and phosphorylation of IκBα protein were not affected by LPS stimulation in the SLAMF1-depleted macrophages (Fig. 3; and Fig. S3 A, lower panels), suggesting that SLAMF1 is not involved in the early NF-κB activation. This is consistent with our data showing that SLAMF1 silencing affected TNF levels only at late time points (Fig. 2).

To further support the hypothesis that SLAMF1 regulates signaling from the endosome leading to *IFNβ* expression, we transduced primary macrophages with lentiviruses encoding SLAMF1. LPS-mediated *IFNβ* mRNA expression was significantly higher in SLAMF1-transduced cells, with only modest effect on *TNF* mRNA expression (Fig. 4 A). Western blot analysis showed that the upregulation of *IFNβ* mRNA expression in SLAMF1 transduced cells was accompanied by higher amounts of phosphorylated TBK1, IRF3 and MAPKs phosphorylation (Fig. 4 B). Thus,

these results also suggest that SLAMF1 acts as a positive regulator of the endosomal TLR4-TRAM-TRIF signaling.

SLAMF1 regulates TRAM recruitment to E. coli phagosomes in a Rab11-dependent manner

Both TLR4 and TRAM are rapidly recruited to *E. coli* phagosomes following phagocytosis, and required for induction of IFNβ (Husebye et al., 2010). Since SLAMF1 was needed for TRAM-TRIF signaling, we tested if SLAMF1 was recruited to *E. coli* phagosomes containing TRAM. We found that TRAM and SLAMF1 were recruited to early (EEA1-positive) and late (LAMP1-positive) *E. coli* phagosomes (Fig. 5 A). This was consistent with the data published for SLAMF1 in mouse macrophages, where SLAMF1 was found both on EEA1- and LAMP1 positive *E. coli* phagosomes (Berger et al., 2010). Moreover, we did not detect SLAMF1 on *S. aureus* phagosomes (Fig. S3 A and B), similarly to the data reported for mouse macrophages (Berger et al., 2010).

We hypothesized that SLAMF1 could be involved in the transport of TRAM to *E. coli* phagosomes as this is a crucial step for TLR4-dependent IFNβ induction. Control and SLAMF1 silenced macrophages were pulsed with *E. coli* pHrodo particles for 15 min, followed by 15 min chase in particle-free medium. The mean voxel intensities (MIs) for TRAM, SLAMF1 and pHrodo fluorescence on the phagosomes were calculated from Z-stacks obtained by confocal microscopy using the 3D-image analysis software (Fig. 5 B). We found that the uptake of *E. coli* particles was not significantly affected by SLAMF1 silencing (Fig. S4 C). However, the acidification of the *E. coli* phagosomes was significantly decreased upon SLAMF1 silencing (Fig. S4 D). Remarkably, we found that TRAM recruitment to *E. coli* phagosomes was markedly decreased upon SLAMF1 silencing (Fig. 5 B, first graph). As expected, SLAMF1 silenced cells showed decreased amounts of SLAMF1 on *E. coli* phagosomes (Fig. 5 B, second graph). Thus, SLAMF1 seems to positively regulate TRAM recruitment to *E. coli* phagosomes.

Transport of TRAM to phagosomes is known to be Rab11-dependent (Husebye et al., 2010). Moreover, SLAMF1 was located to Rab11-positive compartment in resting cells (Fig. 1 C),

positively regulated transport of TRAM to phagosomes (Fig. 5 B) and re-localized from ERC in monocytes upon addition of *E.coli* or LPS (Fig. S4 E-G). Based on these observations we tested if SLAMF1 recruitment to phagosomes was Rab11-dependent. Two members of Rab11 subfamily, Rab11a and Rab11b, were simultaneously silenced in human macrophages. Following silencing, macrophages were stimulated with *E.coli* for 15 and 30 min, and recruitment of TRAM and SLAMF1 to the phagosomes was quantified by evaluating MIs for TRAM and SLAMF1 staining (Fig. 5 C). Rab11 silencing significantly reduced the amounts of SLAMF1 and TRAM at the phagosomes (Fig. 5 C).

SLAMF1 interacts with the N-terminal part of the TRAM TIR domain

To investigate whether TRAM recruitment to *E. coli* phagosomes could be regulated by a physical interaction between SLAMF1 and TRAM, we performed endogenous immunoprecipitations (IPs) using anti-SLAMF1 and anti-TRAM antibodies. Endogenous SLAMF1 co-precipitated with TRAM in macrophages and this interaction was enhanced upon LPS stimulation (Fig. 6 A). In contrast, the TIR-adapter MyD88 did not co-precipitate with SLAMF1 (Fig. 6 A, second panel), supporting the specificity of the SLAMF1-TRAM interaction. Endogenous TRAM also co-precipitated with SLAMF1 both before and after LPS treatment (Fig. 6 B). The bands detected by anti-TRAM antibody were specific as a similar band could be observed in co-IPs with TLR4 upon LPS stimulation (Fig. S5 A). Overall, we conclude that endogenous SLAMF1 interacts with TRAM in human macrophages and the interaction is enhanced upon LPS stimulation.

Further, human embryonic kidney (HEK) 293T cells were transiently transfected with Flag-tagged TRAM ($TRAM^{Flag}$) and full-length SLAMF1 or deletion mutant lacking the C-terminus of SLAMF1 (SLAMF1Δct). We found that full-length SLAMF1, but not SLAMF1Δct co-precipitated with $TRAM^{Flag}$, suggesting that TRAM interaction site was located at the C-terminus of SLAMF1 protein (Fig. 6 C). To map the TRAM region responsible for the interaction with SLAMF1, we

generated several Flag-tagged TRAM deletion mutants. The mutants contained the N-terminus (1-68), C-terminus (158-225), TIR-domain (68-176) or the TIR-domain plus the C-terminus (68-235) of TRAM (1-235, UniProtKB – Q86XR7). Of all the mutants, only TRAM 68-235 and TRAM 68-176 co-precipitated with SLAMF1 (Fig. 6 D).

To further define the sub-domain of TRAM involved in TRAM-SLAMF1 interaction we made a series of TRAM deletion mutants, which contained the N-terminal part of TRAM with 10-20 amino acids (aa) increments. While TRAM 1-68 mutant did not bind SLAMF1 (Fig. 6 D and E), a weak interaction was found with TRAM 1-79 that increased markedly for TRAM 1-90 and further for TRAM 1-100. Taken together, these results suggest that SLAMF1 binding site in TRAM is located within the first 30-35 aa of the TRAM TIR-domain (68-95 aa) (Fig. 6 E).

TRAM interacts with the C-terminal part of SLAMF1 and the interaction occurs for human, but not mouse proteins

We used a similar strategy to establish the TRAM interacting sub-domain of SLAMF1 by deleting aa from the C-terminal part of SLAMF1. Cells were co-transfected with Flag-tagged SLAMF1 WT or deletion mutants along with $TRAM^{YFP}$ (Fig. 6 F). Deletion mutant (1-330) lacking the last 5 C-terminal aa did not interact with $TRAM^{YFP}$ (Fig. 6 F), pinpointing the TRAM interaction site at the very C-terminus of SLAMF1.

There are two tyrosine residues in the cytoplasmic tail of human SLAMF1 in the signaling motifs designated as immunoreceptor tyrosine-based switch motifs (ITSMs) (Shlapatska et al., 2001). SLAMF1 tyrosine phosphorylation and interaction with other proteins via ITSMs could potentially alter SLAMF1-TRAM interaction. Point mutations Y281F, Y327F and double mutation Y281/327F did not alter the interaction with TRAM (Fig. S5 B). Endogenous SLAMF1 was tyrosine phosphorylated in resting macrophages, and subsequently dephosphorylated within the 45 min of LPS stimulation (Fig. S5 C and D). Furthermore, both non-phosphorylated and tyrosine phosphorylated (pY) recombinant SLAMF1ct GST-fusion proteins effectively pulled out TRAM

from lysates of untreated or LPS-treated macrophages (Fig. S5 F). Thus, SLAMF1-TRAM interaction was not altered by tyrosine phosphorylation of SLAMF1.

Regulation of the LPS-induced IFNβ response seems to differ between humans and mice. Human macrophages respond to LPS with at least 10 folds higher IFNβ mRNA expression compared to mouse BMDMs and thioglycollate-elicited peritoneal macrophages (Schroder et al., 2012). Thus, we wanted to check if SLAMF1 and TRAM interaction was conserved across species, and tested murine SLAMF1 and TRAM proteins for interaction. Indeed, mouse $TRAM^{EGFP}$ did not co-precipitate with mouse $SLAMF1^{Flag}$ (Fig. 6 G). Interestingly, three amino acids in human SLAMF1ct upstream of potential TRAM-binding site -TNSI- (321-324, UniProtKB - Q13291) are different from mouse SLAMF1ct, containing -PNPT- (329-332, UniProtKB - Q9QUM4) (Fig. S6 A). Substitution of -TNSI- sequence with -PNPT in human SLAMF1 abrogated its interaction with $TRAM^{YFP}$ (Fig. 6 H). Thus, these amino acids are crucial for interaction. However, the sequence in human TRAM, involved in the interaction with human SLAMF1, is not fully conserved in murine TRAM (Fig. S6 B), which also could explain why murine TRAM and SLAMF1 do not interact.

SLAMF1 has been shown to regulate *E. coli* phagosome maturation in mouse BMDMs, but it did not modify the response to ultrapure LPS (Berger et al., 2010). However, regulation of mRNA expression or secretion of type I IFNs by SLAMF1 have not been previously addressed in BMDMs. We stimulated C57BL/6 *Slamf1*$^{-/-}$ and control BMDMs with 100 ng/ml of ultrapure LPS or *E. coli* particles and tested for *Ifnβ* and *Tnf* mRNA expression and cytokine secretion (Fig. S6 C-E). Indeed, *Slamf1*$^{-/-}$ BMDMs showed comparable *Ifnβ* and *Tnf* mRNA levels to control BMDMs (Fig. S5 C), and the amounts of IFNβ and TNF secreted from *Slamf1*$^{-/-}$ BMDMs stimulated with LPS or *E. coli* were not significantly altered (Fig. S6 D and E). Thus, mouse SLAMF1 does not interact with TRAM protein. Therefore, mouse SLAMF1 did not affect TRAM-TRIF-mediated IFNβ secretion in murine macrophages.

Rab11 interacts with SLAMF1 via class I FIPs

As SLAMF1 recruitment to *E.coli* phagosomes was found to be Rab11 dependent (Fig. 5 C), we investigated if SLAMF1 could form a complex with Rab11 via effector proteins such as Rab11 FIPs (Horgan and McCaffrey, 2009). Individual FIPs (FIP1-5) were co-expressed together with SLAMF1 and $Rab11a^{Flag}$ proteins in HEK cells, followed by co-immunoprecipitation with $Rab11a^{Flag}$ (Fig. 7 A). All three members of class I FIPs were found to form a complex with SLAMF1 and Rab11a (Fig. 7 A). All class I FIPs are characterized by a phospholipid-binding C2-domain (Fig. 7 B), which is located between aa 1 to 129 in FIP2 (Lindsay and McCaffrey, 2004). We found that ΔC2 mutant of FIP2 (lacking 1-128 aa) could still bind SLAMF1 (Fig. 7 D). Protein sequence alignment between the class I FIPs showed a highly conserved domain between aa 117 to 191 in FIP2, with undefined function (Fig. 7 B and C). To figure out if this domain in FIP2 could be responsible for interaction with SLAMF1, several Flag-tagged FIP2 deletion mutants were tested with or without $Rab11^{CFP}$ overexpression. The 1-192 aa deletion mutant was the minimal deletion mutant found to interact with SLAMF1 (Fig. 7 D-F). Both this mutant and the ΔC2 mutant contains a common 62 aa motif that could be important for interaction with SLAMF1 (Fig. 7 D-F).

The tested deletion mutants more efficiently precipitated SLAMF1 than the full length FIP2 (Fig. 7 E), but co-expression of Rab11 with full length FIP2 and SLAMF1 markedly increased its binding to SLAMF1 (Fig. 7 F and G). All FIP2 deletion mutants in IPs lacked C-terminal Rab11 binding domain (RBD) (Fig. 7 B, E, and F), and showed better co-precipitation with SLAMF1 without Rab11 overexpression, which suggested that Rab11 has a critical role in controlling FIP2-SLAMF1 interactions.

Next we examined if FIPs could co-precipitate SLAMF1 efficiently only in the presence of GTP-bound active Rab11. Rab11 GTPase functions as a molecular switch, being active in the GTP-bound state and inactive in the GDP-bound state. It has been shown that FIPs only interact with activated Rab11 (Gidon et al., 2012; Junutula et al., 2004). $FIP2^{Flag}$ was precipitated from cells, which co-expressed SLAMF1 with either Rab11a WT, GTP-bound Rab11Q70L and GDP-bound Rab11a S25N (Fig. 7 G). $FIP2^{Flag}$ co-precipitated with SLAMF1 only in the presence of Rab11 WT

and Rab11Q70L, but not Rab11 SN mutant (Fig. 7 G). We also found that the interaction domain for FIP2 in SLAMF1ct was distinct different from TRAM interaction domain (Fig. 7 I and J; and Fig. 6 F). Our results suggest that TLR4-induced activation of Rab11 is a signal for the recruitment of SLAMF1 and TRAM via the FIPs to *E. coli* phagosomes, and class I FIPs may link the SLAMF1-TRAM complex to Rab11.

SLAMF1 is recruited to the TLR4-TRAM-TRIF complex

We defined the SLAMF1-interacting site in TRAM as the N-terminal part of TRAM TIR-domain (68-95 aa) (Fig. 6 C). This raised an important question whether SLAMF1 could regulate the subsequent formation of TLR4-TRAM-TRIF complex needed for LPS-mediated signaling. To address this question HEK cells were co-transfected by $SLAMF1^{Flag}$, $TRAM^{YFP}$ and $TLR4^{Cherry}$ or $TRIF^{HA}$ and their interactions monitored by co-immunoprecipitation with $SLAMF1^{Flag}$. Both $TLR4^{Cherry}$ and $TRIF^{HA}$ co-precipitated with $SLAMF1^{Flag}$ in the presence of $TRAM^{YFP}$ (Fig. 8 A and B). In addition, SLAMF1 did not co-precipitate with $TLR4^{Flag}$ in the absence of $TRAM^{YFP}$ (Fig. 8 C). Overexpression of SLAMF1 did not alter the ability of TLR4 to attract TRIF via TRAM, despite that SLAMF1 also co-precipitated with the complex in the presence of TRAM and TRIF (Fig. 8 D). Furthermore, TRIF overexpression strongly enhanced SLAMF1 co-precipitation with $TLR4^{Flag}$ (Fig. 8 E). In summary, SLAMF1 binding to TRAM seems to be unique and outside of the TIR-TIR dimerization domain as it does not interfere with TRAM-TLR4 interaction and subsequent TRIF recruitment.

TRAM and SLAMF1 positively regulate bacterial killing by macrophages

SLAMF1 controls killing of Gram-negative bacteria by mouse BMDMs through generation of ROS (Berger et al., 2010). We tested *E. coli*-mediated ROS generation by *SLAMF1*-silenced human macrophages, and found that SLAMF1 also acts as a positive regulator of ROS generation in human cells (Fig. 9 A).

Slamf1$^{-/-}$ BMDMs demonstrated reduced bacterial killing at 6 h of *E. coli* infection (Berger et al., 2010). To test the effect of SLAMF1 on bacterial killing by human cells, *SLAMF1* silenced THP-1 or TRAM knockout (KO) cells with respective control cells were incubated with live DH5α *E. coli*. Bacterial killing was strongly decreased already at early time points (1 h and 1.5 h) in SLAMF1 silenced cells (Fig. 9 B) and almost completely abolished in TRAM KO cells (Fig. 9 C). Negative values of percent of killing in TRAM KO cells pointed to intracellular bacterial replication in these cells (Fig. 9 C).

TRIF-dependent signaling activates TBK1-IKKε kinases that regulate the integrity of pathogen-containing vacuoles and restrict bacterial proliferation in the cytosol (Radtke et al., 2007; Thurston et al., 2016). TRAM is a crucial adapter for TRIF recruitment to activated TLR4, leading to the activation of TBK1 and IKKε (Fitzgerald et al., 2004; Oshiumi et al., 2003; Yamamoto et al., 2003). Upon TLR4 ligation, TBK1 and IKKε phosphorylate Akt kinase (S473), resulting in Akt activation (Everts et al., 2014; Krawczyk et al., 2010). In turn, Akt-mTORC1 signaling axis can drive phagocytosis, phagosome maturation and ROS production, which are essential for bacterial killing (Kelly and O'Neill, 2015). As expected, TRAM KO cells had no detectable IRF3 phosphorylation in response to *E. coli* particles (Fig. 9 D). In control cells, *E. coli*-mediated Akt S473 phosphorylation underwent the similar kinetics as IRF3 phosphorylation, and was completely abolished in TRAM KO cells (Fig. 9 D) and strongly decreased in SLAMF1 depleted cells (Fig. 9 E). TBK1-IKKε inhibitor MRT67307 decreased TLR4-mediated Akt phosphorylation in THP-1 cells, while Akt inhibitor MK2206 completely abrogated Akt phosphorylation (Fig. 9 F). Both compounds inhibited bacterial killing in THP-1 cells, especially at the earliest time point (Fig. 9 G). Moreover, co-incubation with MRT67307 resulted in the increase of intracellular bacterial number as could be seen by negative values in the percentage of bacterial killing (Fig. 9 G).

Hence, TBK1-IKKε activity and subsequent *E. coli*-mediated Akt phosphorylation directly correlated with the ability of cells to kill bacteria and restrict intracellular replication.

Activation of PI3K and subsequent Akt phosphorylation downstream of TLR2 and TLR4 has been extensively explored in many model systems (Laird et al., 2009; Troutman et al., 2012b). It was previously reported that TLR2- and TLR4-mediated Akt S473 phosphorylation is MyD88-dependent in murine model systems (Laird et al., 2009). Our data on MyD88 silencing in primary human macrophages showed that *E. coli*-induced Akt S473 phosphorylation was not dependent on MyD88, but dependent on TRAM (Fig. S7 A). In human macrophages the kinetics of Akt phosphorylation induced by *E. coli* particles was much faster and robust than induced by the TLR2 ligand FSL-1, or the TLR4 ligand, LPS (Fig. S7 B). TLR2 and TLR4 ligands were not inducing pAkt much over the background level in THP-1 cells that were used for bacterial killing assays, and pAkt levels were only modestly affected by *SLAMF1* or *TRAM* silencing (Fig. S7 C). In contrast, THP-1 cells stimulated with *E. coli* particles showed a 15-20 fold increase in pAkt that were almost lost in cells depleted for *TRAM* or *SLAMF1* (Fig. 9 D and E). Thus, TRAM and SLAMF1 are involved in regulation of *E. coli*-mediated, but not pure TLR ligands-mediated, Akt phosphorylation in THP-1 cells.

Discussion

Despite that SLAMF1 has been reported to control inflammatory responses and defense against Gram-negative bacteria in mice, the underlying mechanisms are elusive (Theil et al., 2005; van Driel et al., 2012; van Driel et al., 2016). Moreover, little has been shown about the role of SLAMF1 in modulating the inflammatory response against Gram-negative bacteria in human macrophages. Here we show for the first time that human SLAMF1 regulates TLR4-mediated TRAM-TRIF-dependent signaling by the unique interaction with the signaling adapter TRAM.

Mouse BMDMs express high levels of SLAMF1 on the plasma membrane, whereas resting human monocytes and human monocyte-derived macrophages has been considered being SLAMF1-negative (Farina et al., 2004; Romero et al., 2004). In contrast, we found that human monocytes and macrophages largely expressed SLAMF1 in the intracellular $Rab11^+$ ERC

compartment, however with weak or no expression on the cell surface. Following stimulation by *E. coli*, SLAMF1 re-localized from ERC to *E. coli* or LPS containing phagosomes that resembled the previously reported Rab11a-dependent transport of TLR4 and TRAM from ERC to *E. coli* phagosomes (Husebye et al., 2010). Endogenous SLAMF1 was already bound to TRAM before stimulation, and upon *E.coli* phagocytosis both proteins were recruited to phagosome by Rab11 GTPases with class I Rab11 FIPs as effector molecules. It is known that Rab11 functions as a molecular switch, which cycles between two conformational states: a GTP-bound 'active' form and a GDP-bound 'inactive' form (Guichard et al., 2014). Surface TLR4 interaction with LPS on *E.coli* outer membrane induces fast intracellular complex formation resulting in multiple posttranslational modifications of signaling molecules (Mogensen, 2009). We hypothesize that TLR4 signaling results in a shift of Rab11 GDP-bound to Rab11 GTP-bound active state. Moreover, previous reports have demonstrated that FIPs prefer binding to GTP-bound Rab11 (Junutula et al., 2004). Thus, after Rab11 GDP/GTP ratio shifts to GTP-bound state, FIPs would connect cargo to Rab11 vesicles, which would enhance delivery of SLAMF1 and TRAM – via FIPs class I from ERC to *E.coli* phagosomes.

Mouse SLAMF1 is shown to be a bacterial sensor by itself, recognizing porins in the outer bacterial membrane (Berger et al., 2010). The regulatory role of mouse SLAMF1 upon TLR4 ligation by LPS is directly dependent on the porins present in crude LPS preparations or porins in the bacterial outer membrane (Berger et al., 2010). Unlike its mouse orthologue, human SLAMF1 did not require interaction with bacterial porins to elicit its effects on TLR4-mediated IFNβ production, as similar data were obtained with both *E. coli* bioparticles and ultrapure LPS.

The delivery of TRAM to endosomes and phagosomes is crucial for the activation of IRF3 signaling pathway and IFNβ induction (Husebye et al., 2010; Kagan et al., 2008). We found that SLAMF1 silencing caused a significant decrease in TRAM accumulation around *E. coli* phagosomes. Moreover, endogenous TRAM co-immunoprecipitated with SLAMF1. These data demonstrate that SLAMF1 is a critical regulator of TRAM recruitment to the phagosomes. We were

able to map the domain in SLAMF1 involved in interaction with TRAM to 15 C-terminal amino acids, since both deletion of 5 C-terminal amino acids and substitution of amino acids at positions 321-324 abrogated interaction of SLAMF1 protein with TRAM. Interaction domain in TRAM was located outside the BB loop as TIR-TIR dimerization is not affected, and mapped to the N-terminal part of TRAM TIR-domain between amino acids 68 to 95. We found that mouse SLAMF1ct contains different amino acid sequence at positions corresponding to human 321-324 residues. This resulted in the absence of interaction between mouse SLAMF1 and TRAM, and consequently LPS- or *E. coli*-induced IFNβ expression was not altered in *Slamf1*$^{-/-}$ BMDMs when compared to WT cells.

The failure to activate TBK1-IKKε kinase observed upon SLAMF1 silencing may affect the anti-bacterial functions of TBK1-IKKε (Radtke et al., 2007; Thurston et al., 2016). The Akt kinase, which is activated by TBK1-IKKε upon TLR4 ligation, is directly involved in TLR4-mediated switch to glycolysis by phosphorylating crucial downstream target proteins (Kelly and O'Neill, 2015; Krawczyk et al., 2010). Moreover, Akt is involved in activation of NADPH oxidase by phosphorylating p47(PHOX) subunit (Chen et al., 2003; Hoyal et al., 2003) that may result in ROS generation needed for bacterial killing (West et al., 2011). We demonstrate that SLAMF1 and TRAM were required for *E. coli*-mediated Akt phosphorylation via TBK1-IKKε as well as for the efficient bacterial killing. It is known that TLR2 and TLR4 ligands activate Akt S473 in a MyD88-dependent manner (Laird et al., 2009; Troutman et al., 2012b). It should be noted that in contrast to these studies, we have used *E. coli* particles and found that Akt S473 phosphorylation was TRAM and SLAMF1 dependent. Akt phosphorylation induced by pure TLR2 and TLR4 ligands could be more dependent on MyD88-, but was not dependent on SLAMF1- or TRAM in THP-1 macrophages.

There is accumulating evidence on divergent regulation of TLR4 signaling and gene expression in different species (Schroder et al., 2012; Vaure and Liu, 2014). It is known that humans and old world monkey species are highly sensitive to LPS with physiological changes

induced by a dose at nanogram per kilogram, whereas rodents are highly insensitive to LPS with physiological changes only induced by a dose at milligrams per kilogram (reviewed in (Vaure and Liu, 2014)). Many therapeutic agents that reduce inflammation and mortality in mouse septic shock models show no clinical benefit for humans (Poli-de-Figueiredo et al., 2008). Human monocyte-derived macrophages express much higher levels of *IFNβ* mRNA in response to LPS than mouse BMDM or thioglycollate-elicited peritoneal macrophages (Schroder et al., 2012). Our findings support higher LPS-induced secretion of IFNβ by human macrophages compared to BMDMs. Thus, during evolution human macrophages must have acquired mechanisms to enhance TLR4-mediated IFNβ production in response to LPS, or vice versa, mouse cells developed less sensitive response to bacterial LPS. We suggest that SLAMF1-regulated transport of TRAM to TLR4 signaling complex on bacterial phagosomes could be one of the features specific for human cells, which amplifies the IFNβ secretion. Thus, human SLAMF1 could potentially be targeted to regulate TLR4-mediated cytokine production in inflammatory conditions.

MATERIALS AND METHODS

Primary cells and cell lines

Use of human monocytes from blood donors was approved by the Regional Committees from Medical and Health Research Ethics at NTNU. Human monocytes were isolated from buffycoat by adherence as previously described (Husebye et al., 2010). Briefly, freshly prepared buffycoat (The Blood Bank, St Olavs Hospital, Trondheim, Norway) was diluted by 100 ml of PBS, and applied on top of Lymphoprep (Axis-Shield) according to manufacturer's instructions. PBMCs were collected and washed by Hank's Balanced Salt Solution (Sigma) 4 times with low speed centrifugation (150-200 g). Cells were counted using Z2 Coulter Particle Count and Size Analyzer (Beckman Coulter) on program B, re-suspended in RPMI1640 (Sigma) supplemented with 5% of pooled human serum at concentration of 8 x 10^6 per ml and seeded to 6-well (1 ml per well) or 24-well (0.5 ml per well) cell culture dishes. Following a 45 min incubation, allowing surface adherence of monocytes, the dishes were washed 3 times by Hank's Balanced Salt Solution to remove non-adherent cells. Monocytes were maintained in RPMI1640 supplemented with 10% of pooled human serum (The Blood Bank, St Olavs Hospital, Trondheim, Norway) and used within 24 h after isolation. Monocyte-derived macrophages were obtained by differentiating cells for 8-10 days in RPMI1640 with 10% human serum and 25 ng/ml rhM-CSF (#216-MC-025, R&D Systems). THP-1 cells (ATCC), cultured in RMPI1640 supplemented by 10% heat inactivated FCS, 100 nM penicillin/streptomycin (Life Technologies) and 5 μM β-mercaptoethanol (Sigma). THP-1 cells were differentiated with 50 ng/ml of phorbol 12-myristate 13-acetate (PMA) (Sigma) for 72 h, followed by 48 h in medium without PMA. HEK293T (ATCC) were cultured in DMEM with 10% FCS. For making TRAM KO THP-1 cell line, LentiCRISPRv2 plasmid (Sanjana et al., 2014) (gift from Feng Zhang lab - Addgene #52961) was ligated with 5′-CACCGATGACTTTGGTATCAAACC-3′ and 5′- AAACGGTTTGATACCAAAGTCATC-3′ for TRAM. Packaging plasmids pMD2.G and psPAX2 were used for producing lentivirus (kindly provided by TronoLab, Addgene plasmid # 12260, #12259). HEK293T cells were co-transfected

with the packaging and lentiCRISPRv2 plasmids, and washed after 16 h. The lentivirus containing supernatants were collected after 48 h, and used for transduction of THP-1 cells along with 8 μg/ml protamine sulphate. Transduced THP-1 cells were then selected with Puromycin (1 μg/ml) for 1 month, and tested for TRAM protein expression by Western blot. All cell lines were regularly checked for mycoplasma contamination.

Reagents and cell stimulation

pHrodo Red *E. coli* and *S. aureus,* AF488-conjugated *E. coli* bioparticles were purchased from Thermo Fisher Scientific. Ultrapure 0111:B4, K12 LPS from *E. coli*, polyinosinic-polycytidylic acid [poly(I:C)], imidazoquinoline compound R848 (Resiquimod), thiazoloquinoline compound CL075, synthetic diacylated lipoproteins FSL-1 (Pam2CGDPKHPKSF) and Pam3CSK4 (P3C) were from InvivoGen. Ultrapure K12 LPS or 0111:B4 LPS (InvivoGen) were used at concentration 100 ng/ml. *E. coli* bioparticles were reconstituted in 2 ml PBS, and 50 μl/well (1.5 x 10^7 particles) in 1 ml of media was used for cells in 6-well plates (NUNC) or 35-mm glass bottom tissue cell dishes (MatTek Corp.), 15 ul/well (0.45 x 10^7 particles) in 0.5 ml of media – for 24-well plates (NUNC). Pan-Akt inhibitor MK2206 (#1032350-13-2, Axon Medchem) and TBK1-IKKε inhibitor MRT67307 (from Prof. Philip Cohen, University of Dundee, United Kingdom) (Clark et al., 2011) were diluted in DMSO at concentration 20 mM and stored at -80 ^{o}C, working solutions prepared in cell culture media immediately before use.

Antibodies

The following primary antibodies were used: rabbit-anti-TICAM-2/TRAM (GTX112785) from Genetex; rabbit mAbs anti-human SLAMF1/SLAMF1 (#10837-R008-50) from Sino Biological Inc.; mouse anti-GAPDH (ab9484), rabbit anti-phospho-IRF3 Ser386 (ab76493) from Abcam; rabbit anti phospho-Akt Ser473 (D9E) #4060, phospho-IRF3 Ser396 (4D4G) #4947, IkB-α (44D4) #4812, phospho-IkB-α (14D4) #2859, p38 MAPK #9212, phospho-p38 MAPK (Thr180/Tyr182)

(D3F9) #4511, TBK1/NAK (D1B4) #3504, phospho-TBK1/NAK (Ser172) (D52C2) #5483, phospho-TAK1 (T184/187) (90C7) #4508, TAK1 #5206, phospho-SAPK/JNK (Thr183/Tyr185) (81E11) #4668, anti-DYKDDDDK Tag (D6W5B)/Flag-tag #14793, anti-MyD88 (D80F5) #4283, phospho-STAT1 (Tyr701) (D4A7) #7649 from Cell Signaling; rabbit anti total IRF3 (FL-425) # sc-9082, PCNA (FL-261) #sc-7907 were from Santa Cruz Biotech; Living Colors rabbit anti full-length GFP polyclonal Abs (#632592) from Clontech; 4G10® Platinum anti-phosphotyrosine antibody biotin conjugated (#16-452) were from MerkMillipore (Merck Life Science AS); mouse anti-Glutathione-S-Transferase Abs (SAB4200237), monoclonal mouse ANTI-FLAG M2 antibodies (#F1804-200UG) from Sigma. Secondary antibodies (HRP linked) for Western blotting were swine anti-rabbit (P039901-2) and goat anti-mouse (P044701-2) from DAKO/Agilent. The following antibodies were used for staining and/or IPs: rabbit anti-LAMP1 (ab24170), GM130 antibody [EP892Y] cis-Golgi marker (ab52649) from Abcam; rabbit anti EEA1 (H-300) #sc-33585, TICAM2/TRAM (H-85), TLR4 (H-80) #sc-10741, normal rabbit IgG (#sc-2027), normal mouse IgG (#sc-2025) from Santa Cruz Biotech; rabbit anti-Rab11, LEAF^{TM} purified mouse IgG1 isotype control (MOPC-21) # 400124, LEAF^{TM} purified mouse anti-CD150 (SLAMF1) A12 (7D4) #306310 from Biolegends; anti-SLAMF1 IgG1 (IPO-3) kindly provided by Sidorenko S.P. (IEPOR NASU, Kyiv, Ukraine) (Sidorenko and Clark, 1993). Secondary antibodies for confocal microscopy: goat anti-mouse IgG (H+L) Alexa Fluor® 405 conjugate (A-31553), Alexa Fluor® 488 conjugate (A-11001), Alexa Fluor® 647 conjugate (A-21235), goat anti-rabbit IgG (H+L) Alexa Fluor® 405 conjugate (A-31556), Alexa Fluor® 488 conjugate (A-11008) and DNA stain Hoechst 33342 (#62249) from Thermo Fisher Scientific.

Imaging and image analysis

Confocal images were captured using either a Zeiss LSM 510 META (Carl Zeiss) equipped with a plan-apochromat 1.4 NA × 63 oil-immersion objective (images presented on Fig. 1A and used for 3D modeling on Fig. 1B), or Leica TCS SP8 (Leica Microsystems) equipped with HC PL APO

63x/1.40 Oil CS2 objective. Fluorescence was captured by standard PMT detectors (Zeiss LSM 510 META), or STED HyD or PMT detectors (Leica TCS SP8). Acquisition software for Zeiss LSM 510 META was Zeiss Zen 2012 Microscope Software (Carl Zeiss Microscopy), and LAS AF Sotware 4.0.0.11706 (Leica Microsystems CMS GmbH) for Leica TCS SP8. Prior imaging, cells were fixed with 2% paraformaldehyde in PBS on ice, immunostaining was performed as described (Husebye et al., 2010). Briefly, upon fixation the cells were permeabilized with PEM buffer (80 mM K-Pipes [pH 6.8], 5 mM EGTA, 1 mM MgCl2, 0.05% saponin) for 15 min on ice, quenched of free aldehyde groups in 50 mM NH4Cl with 0.05% saponin for 5 min, and blocked in PBS with 20% human serum and 0.05% saponin. The cells were incubated with primary antibody in PBS with 2% human serum and 0.05% saponin overnight at 4 °C, or for 2 hours at RT. Alexa Fluor-labeled secondary antibodies (Invitrogen/Thermo Fisher Scientific) were incubated 15 min at room temperature after three washes in PBS with 0.05% saponin. If double staining was made, cells were sequentially stained by first primary Abs, specific secondary Alexa Fluor-conjugated Abs, second primary Abs, specific secondary Alexa Fluor-conjugated Abs. Images of stained cells, washed in PBS with 0.05% saponin and left in PBS, were captured at RT. 3D data were captured with identical settings, which were also adjusted to avoid saturation of voxels (3D pixels) intensities. For co-localization analysis, Coloc 2 plugin with thresholds in ImageJ/Fiji application was applied (Schindelin et al., 2012). The pHrodo fluorescence was used to spot or surface render the volume of individual phagosomes when *E. coli* pHrodo or *S. aureus* pHrodo red, or AF488-conjugated *E. coli* particles were used. Binary mask was created around bacterial particles (Process/Make Binary function), and used to define the regions for quantification of mean intensities (MI) for TRAM and SLAMF1 voxels in original images, and to quantify *E. coli* pHrodo particles MI when re-directed to the original image. *E. coli* pHrodo MI was evaluated to quantify acidification of *E. coli*-containing phagosomes in cells treated by control or *SLAMF1* siRNA. For analysis of sum of voxel intensities of SLAMF1 inside Golgi rings, GM130 staining was used to define the region to evaluate SLAMF1 intensities for individual 3D Golgi ring structure. Using ImageJ/Fiji software, 3D Golgi ring

structures were selected as region of interest (ROI) and used as a mask to obtain a numerical value of the relative amount of SLAMF1 as a sum of voxel intensities for SLAMF1 staining in Golgi rings ROI from original image. The ImarisXT software (Bitplane) was used to surface render the imaged GM130-positive structures giving one surface for each. The values for voxel intensities did not follow a Gaussian distribution, and therefore we used median as a measure of average intensities and the nonparametric Mann-Whitney test to evaluate statistical significance in GraphPad Prizm 5.03 (GraphPad Software).

siRNA Treatment

Oligos used for silencing were AllStars Negative Control siRNA SI03650318, FlexiTube siRNA Hs_SLAMF1_2 SI00047250, Hs_MYD88_2 SI00038297, HS_TICAM2_2 SI00130893, Hs_RAB11A_5 SI00301553 together with Hs_RAB11B_6 SI02662695 (Qiagen). On day 7 cells were transfected by silencing oligo (20 nM final concentration) using Lipofectamine 3000 #L3000008 from Invitrogen/Thermo Fisher Scientific as suggested by manufacturer. Cells were stimulated by LPS or *E. coli* particles for 96 h after transfection. For THP-1 cells, cells were seeded in 6-well plates (NUNC) 0.4 x 10^6 per well, in antibiotic-free media supplemented by 40 ng/ml of PMA. Transfection of siRNA was performed in 24 h, media was changed to PMA-free in 72 h, and cells were kept for another 48 h before stimulation by LPS or *E.coli* particles.

Q-PCR

Total RNA was isolated form the cells using Qiazol reagent # 79306 from QIAGEN, and chloroform extraction followed by purification on RNeasy Mini columns with DNAse digestion step (Qiagen). cDNA was prepared with Maxima First Strand cDNA Synthesis Kit for quantitative real-time polymerase chain reaction (RT-qPCR) (ThermoFisher Scientific) according to the manufacturer's protocol. Q-PCR was performed using the PerfeCTa qPCR FastMix (Quanta Biosciences) in replicates, and cycled in a StepOnePlus™ Real-Time PCR cycler. The following

TaqMan® Gene Expression Assays (Applied Biosystems®) were used: *IFNβ* (Hs01077958_s1), *TNF* (Hs00174128_m1), *SLAMF1* (Hs00900288_m1), *TBP* (Hs00427620_m1), *CXCL10* (Hs01124251_g1), *Rab11a* (Hs00366449_g1), *Rab11b* (Hs00188448_m1) for human cells; *Ifnβ* (Mm00439552_s1), *Tnf* (Mm00443258_m1), *Tbp* (Mm01277042_m1) for mouse cells. No-RT controls were negative. The level of *TBP* mRNA was used for normalization and results presented as relative expression compared to the control untreated sample. Relative expression was calculated using the Pfaffl's mathematical model (Pfaffl, 2001). Results presented as mean and SD expression fold change for biological replicates relative to non-stimulated cells. Statistical significance was evaluated in GraphPad Prizm 5.03. Data distribution was assumed to be normal but this was not formally tested. The difference between the two groups was determined by the two-tailed *t* test.

Cloning, expression vectors and DNA transfection

Phusion High-Fidelity DNA Polymerase and respective Fast Digest enzymes (Thermo Fisher Scientific) were used for cDNA re-cloning. Plasmids we purified by Endofree plasmid Maxi kit (QIAGEN). Sequencing of plasmids was done at Eurofins Genomics facility, Germany. Primers for cloning are listed below. *SLAMF1* coding sequence was re-cloned from retroviral vector (from A. Taranin, Novosibirsk, Russia) to pcDNA3.1 (Invitrogen), C-terminal-DYKDDDDK (Flag-tag) vector (Clontech), deletion mutants of SLAMF1 made in pcDNA3.1 vector or C-terminal-DYKDDDDK vector. Human $TRIF^{HA}$ and $TRAM^{YFP}$ from K. Fitzgerald (University of Massachusetts Medical School, Worcester, MA, USA) were used for transfections or as template for re-cloning and making TRAM deletion mutants. $Rab11a^{Flag}$ coding construct described (Klein et al., 2015); Rab11FIP1, ΔC2 Rab11FIP2, Rab11FIP2, Rab11FIP3, Rab11FIP4, Rab11FIP5 in pEGFPC1 vector were from M. McCaffrey (Biosciences Institute, University College Cork, Ireland). Rab11aQ70L and Rab11aS25N were PCR amplified from pEGFP-Rab11Q70L and pEGFP-Rab11aS25N (Husebye et al., 2010), respectively. The amplified fragments were inserted into SalI and BamHI restricted pECFP-C1 vector. TLR4 was re-cloned from $TLR4^{Cherry}$ construct

(Husebye et al., 2010) to C-terminal-DYKDDDDK vector. Mouse SLAMF1 was re-cloned to C-terminal-DYKDDDDK vector, mouse TRAM was re-cloned from GeneScript ORF clone (OMu22478D) to pEGFP-N1 vector (Clontech). pDUO-hMD-2/CD14 (Invivogen) was co-expressed with TLR4 to ensure TLR4 dimer formation. HEK 293T cells in 6-well plates were transfected by 0.2-0.4 ug of vectors/well using Genejuice transfection reagent (Millipore). Lysates were prepared 48 h after transfection. Primers used for cloning are listed in Table 1.

Immunoprecipitations

HEK293T cells expressing Flag-tagged proteins, or macrophages for endogenous IPs were lysed using 1 X lysis buffer (150 mM NaCl, 50 mM TrisHCl (pH 8.0), 1 mM EDTA, 1% NP40), or 1 X lysis buffer with high salt (400 mM NaCl, 50mM TrisHCl (pH7.5), 1% Triton X100, 5 mM EDTA) for anti-phosphotyrosine IPs), supplemented with EDTA-free Complete Mini protease Inhibitor Cocktail Tablets and PhosSTOP phosphatase inhibitor cocktail from Roche, 50 mM NaF and 2 mM Na_3VO_3 (Sigma). IPs were carried out by rotation at 4 ^oC for 2 hs of cell lyastes with either anti-flag (M2) agarose (Sigma) or specific antibodies coupled to Dynabeads (M-270 Epoxy, Thermo Fisher Scientific), or phosphotyrosine biotinylated antibodies on streptavidin beads (Invitrogen). Agarose, sepharose or Dynabeads were washed 5 times by respective lysis buffers, heated for 5 min with 1X NuPAGE® LDS Sample Buffer (Thermo Fisher Scientific) for agarose and sepharose beads or eluted by Elution buffer (from Dynabeads co-immunoprecipitation kit #14321D, Thermo Fisher Scientific) for Dynabeads before analysis by Western blotting.

Western blotting

Cell lysates, other than used as controls in immunoprecipitations, were prepared by simultaneous extraction of proteins and total RNA using Qiazol reagent (Qiagen) as suggested by manufacturer. Protein pellets were dissolved by heating protein pellets for 10 min at 95 ^oC in buffer containing 4 M urea, 1% SDS (Sigma) and NuPAGE® LDS Sample Buffer (4X) (Thermo Fisher Scientific).

Otherwise, lysates were made using 1X RIPA lysis buffer (150 mM NaCl, 50mM TrisHCl (pH7.5), 1% Triton X100, 5 mM EDTA, protease inhibitors, phosphatase inhibitors). For Western blot analysis we used pre-cast protein gels NuPAGE™ Novex™ and iBlot Transfer Stacks iBlot Gel Transfer Device (ThermoFisher Scientific).

Lentiviral transduction

For making TRAM KO cell line, LentiCRISPRv2 plasmid (gift from Feng Zhang lab - Addgene #52961) was ligated with 5′-CACCGATGACTTTGGTATCAAACC-3′ and 5′-AAACGGTTTGATACCAAAGTCATC-3′ for TRAM. The second-generation packaging plasmids pMD2.G and psPAX2 were used for producing lentivirus (kindly provided by TronoLab, Addgene plasmid # 12260, #12259). HEK293T cells were co-transfected with the packaging and lentiCRISPRv2 plasmids, and washed after 16 h. The lentivirus containing supernatants were collected after 48 h, and used for transduction of THP-1 wt cells along with protamine sulphate (8 μg/ml final concentration). Transduced THP-1 cells were selected with Puromycin (1 μg/ml) for 1 month, and tested for TRAM protein expression by Western blot. Lentivirus construct of SLAMF1 was prepared by cloning full size SLAMF1 with or without Flag tag to the bicistronic lentiviral expression vector pLVX-EF1α-IRES-ZsGreen1 (Clontech) (primers listed in Table 1). Construct was sequenced and co-transfected with packaging plasmids (psPAX2 and pMD2.G, kindly provided by TronoLab, Addgene plasmid #12260, #12259) to produce pseudoviral particles in HEK293T cells. Supernatants were collected in 48 and 72 h, combined, and concentrated using Lenti-X™ Concentrator (#631231) from Clontech. Viral particles were titrated in HEK293T cells. Titrated virus particles, which gave 90-100% of transduction efficiencies, were subsequently used for transduction of primary human macrophages (resulting in 30 to 40% of ZsGreen positive cells). Macrophages were infected on day 6 of differentiation, media changed in 24 h, stimulation by LPS (100 ng/ml) performed in 72 h after transduction. Cell lysates for simultaneous RNA/protein isolation were prepared using Qiazol reagent.

Flow cytometry

Untreated or LPS-stimulated monocyte-derive macrophages were detached using accutase (A6964) from Sigma, and stained with a cocktail of antibodies against human CD14 (MΦP9) FITC conjugated from BD Biosciences and SLAMF1 IgG1 (IPO-3) mAbs labeled by AF647 using Alexa Fluor® 647 Protein Labeling Kit (A20173), for 30 min on ice. Flow cytometry was performed using LSR II (BD Biosciences) with FACS Diva software (BD Biosciences). Samples were analyzed with FlowJo 7.6 software (TreeStar).

ELISA and Multiplex Cytokine Assay

TNF in supernatants was detected using a human TNF-alpha DuoSet ELISA (DY210-05) (R&D Systems), IFNβ level – using VeriKine-HSTM Human Interferon-Beta Serum ELISA Kit (#41415) from PBL Assay Science. Supernatants were also analyzed by multiplex cytokine assay (Bio-Plex; Bio-Rad Laboratories Inc.) for IL-1β, IL-6, IL-8, CXCL-10/IP-10. TNF in BMDMs supernatants was detected using mouse TNF-alpha DuoSet ELISA (DY410-05) from R&D Systems, IFNβ level accessed using VeriKine-HS Mouse Interferon Beta Serum ELISA Kit (#42410-1) from PBL Assay Science. Results presented as mean and SD for biological replicates for representative donor (primary human macrophages), or at least three independent experiments for model cell line THP-1. Statistical significance was evaluated in GraphPad Prizm 5.03. Data distribution was assumed to be normal but this was not formally tested. The difference between the two groups was determined by the two-tailed *t* test.

Blocking IFN receptor by specific antibodies

Differentiated THP-1 cells in 6-well plates were incubated for 30 min at 37 ^{o}C with 2.5 μg/ml with anti-Interferon-α/β receptor chain 2 antibodies, clone MMHAR-2 isotype IgG2a (#MAB1155) from Millipore/MERCK or control monoclonal antibodies (mAbs) Leaf^{TM} purified mouse IgG2a κ isotype MOPC-173 (#400224) from BioLegends. Following pre-incubation with mAbs, cells were

stimulated with LPS (100 ng/ml) and lysed using Qiazol reagent (Qiagen) for simultaneous extraction of proteins and total RNA.

GST pulldown assays

GST-fusion protein construct of SLAMF1ct (GST-SLAMF1ct) was prepared by cloning SLAMF1ct (corresponding to 259-335 aa of SLAMF1 protein, UniProt Q13291) to pGEX-2TK vector (GE Healthcare Life Sciences). Sequenced plasmid was transformed into the BL21 DE3 bacterial strain (New England Biolabs) or to TKX1 strain (Agilent Technologies) for production of tyrosine-phosphorylated GST-SLAMF1ct-PY. Expression and purification of GST fusion proteins were performed as described (Shlapatska et al., 2001). For protein purification and for pull down assays we used Glutathione High Capacity Magnetic Agarose Beads (G0924) from Sigma. Cell lysates of untreated and LPS stimulated macrophages were prepared in 1 X lysis buffer (0.5% NP40 (Nonidet-P40), 150 mM NaCl, 50 mM TrisHCl (pH 8.0). Pull downs were performed as described earlier (Shlapatska et al., 2001).

Mouse BMDMs differentiation and stimulation

All protocols on animal work were approved by the Norwegian National Animal Research Authorities and were carried out in accordance with Norwegian and European regulations and guidelines. Bone marrow-derived macrophage cultures were generated from bone marrow aspirates extracted from the femurs of C57BL/6 mice 8-10 weeks old male control mice or from *Slamf1*$^{-/-}$ C57BL/6 mice (Wang et al., 2004). Cells were cultured in complete RPMI-1640 medium containing 20% of L929 conditioned media produced in-house for 8–10 days in sterile bacterial Petri dishes; cells were counted and seeded to 24-well cell culture plates in RPMI-1640 with 10% FCS at concentration 0.3 x 10^6 per well in triplicate, left overnight and treated next day in fresh media by 100 ng/ml UP LPS (Invivogen) or 50 µg/well for 6-well plate or 20 ug/well for 24-well plate of

E.coli particles. Cell lysates for RNA isolation were made using Qiazol reagent (#79306) from QIAGEN.

ROS activation assay

Primary human macrophages (in 6 well plates) were treated by siRNA as described, and treated by *E. coli* red pHrodo bacterial particles (excitation wavelength 561 nm) in 0.5 ml RPMI1640 containing 10% human serum on water bath (for 20 min incubation) or in CO_2 incubator (for 120 min incubation). Freshly dissolved in washing buffer (reagent A) dihydrorhodamine 123 (DHR-123, excitation wavelength 488 nm) (reagent E), both from PHAGOBURST kit (Glycotope Biotechnology), was added to the wells (except for control well, washing buffer added) for the last 10 min of incubation. After stimulation, cells were placed on ice, washed by cold PBS, incubated with accutase (Sigma) on ice for 5 min, and scraped using cell scrapers. Cells were washed by flow wash (PBS with 0.5% FCS), fixed by fixation buffer (BD Biosciences), washed by PBS, and analyzed by flow cytometry using LSR II (BD Biosciences) with FACS Diva software (BD Biosciences). In FlowJo 7.6 software (TreeStar) cells were gated for pHrodo-positive cells, and DHR-123 fluorescence was presented on the graphs for this gate.

Bacterial killing assay

THP-1 cells were plated at $2x10^5$ cells/well in 24-well plates and differentiated as described previously for 5 days. Cells were washed and transferred to serum-free RPMI medium. DH5α *E. coli* were added at a multiplicity of infection (MOI) of 40. *E. coli* were centrifuged onto differentiated THP-1 monolayers at 2000 rpm for 5 min at 4 ^oC. Plates were warmed to 37 ^oC for 15 min in a water bath. Each well was then washed 3 X with ice-cold PBS and incubated with warm 10% FCS RPMI medium containing 100 μg/ml of gentamycin for 30 min at 37 ^oC to remove extracellular bacteria. If inhibitors were used in the assay, either DMSO or inhibitors were added to the media at designated concentrations. Cells were washed again 2 X with PBS. This time point (45

min after adding bacteria) was designated as time 0. To measure colony forming unit (CFU) at the end of incubation time, triplicate wells were washed and lysed in 1 ml sterile water. Plates for time points 1 h and 1.5 h were further incubated at 37 ^{o}C, CO_2 incubator in medium with 10% FCS, without antibiotics, with or without kinase inhibitors. At each time point, triplicate wells were washed 3 X with PBS before lysing the cells. Viable counts were determined by plating 10 µl of 10-fold fold dilutions, $1:10^2$ and $1:10^3$ onto LB agar (in triplicates to account for technical pipetting error). CFU was counted at each time point including time 0. Percent killing was calculated = 100 - [(#CFU at time X / #CFU at time 0) x 100] for average values of technical replicates. Statistical significance calculated in GraphPad Prizm 5.03 for biological replicates using unpaired two-tailed test.

Online supplemental material

Fig. S1 shows that LPS treatment induces SLAMF1 expression in human cells resulting in its surface localization, and the increase in SLAMF1 expression is not dependent on signaling from the IFNα/β receptor. Fig. S2 shows that SLAMF1 is involved in regulation of *E. coli*- or LPS-mediated, but not TLR3-, TLR8- or RIG-I/MDA5- mediated, *IFNβ* or *TNF* mRNA expression. Fig. S3 shows that knockdown of SLAMF1 in THP-1 cells impairs TLR4-mediated phosphorylation of TBK1, IRF3 and TAK1 in response to LPS or *E. coli* particles. Fig. S4 shows that SLAMF1 re-localizes from ERC to early and late *E. coli* phagosomes, but not *S. aureus* phagosomes, and is required for *E. coli* phagosome acidification in human cells. Fig. S5 shows that SLAMF1 interaction with TRAM is independent from SLAMF1 tyrosine phosphorylation. Fig. S6 shows that TLR4-mediated *IFNβ* and *TNF* mRNA expression and corresponding cytokine secretion are not altered in *Slamf1*$^{-/-}$ BMDMs, and provides human and murine SLAMF1 and TRAM proteins sequences alignments. Fig. S7 shows that *E. coli*-mediated Akt phosphorylation in human macrophages is not dependent on MyD88 expression, and TLR2- and TLR4-induced phosphorylation of Akt is weak and not much dependent on *SLAMF1* or *TRAM* expression.

Acknowledgments

We thank S. Sidorenko (IEPOR, Kiev, Ukraine), V. Kashuba (KI, Stockholm, Sweden) and M. McCaffrey (University College Cork, Ireland) for providing reagents and V. Boyartchuk (NTNU, Trondheim, Norway) for expert advice. Confocal imaging was performed at the Cellular and Molecular Imaging Core Facility, Norwegian University of Science and Technology (NTNU). This work was supported by the Research Council of Norway through its Centers of Excellence funding scheme Grant 223255/F50 (to T.E.), NTNU's Onsager Fellowship (to R.K.K), and by grants from the Liaison Committee for education, research and innovation in Central Norway (to T.E.), and Joint Research Committee between St. Olavs Hospital and Faculty of Medicine and Health Science, NTNU (to H.H.). The authors declare no competing financial interests.

Author contributions

Conceptualization, M.Y, H.H. and T.E.; Methodology, M.Y., H.H., A.S. and T.E.; Investigation, M.Y., A.S., L.R., H.H., G.M.R., and N.W.; Writing – Original Draft, M.Y.; Writing – Review & Editing, M.Y., A.S., H.H., C.T., and T.E.; Supervision, H.H. and T.E.; Resources, R.K.K., C.T. and N.W.

References

Avota, E., E. Gulbins, and S. Schneider-Schaulies. 2011. DC-SIGN mediated sphingomyelinase-activation and ceramide generation is essential for enhancement of viral uptake in dendritic cells. *PLoS Pathog*. 7:e1001290.

Berger, S.B., X. Romero, C. Ma, G. Wang, W.A. Faubion, G. Liao, E. Compeer, M. Keszei, L. Rameh, N. Wang, M. Boes, J.R. Regueiro, H.C. Reinecker, and C. Terhorst. 2010. SLAM is a microbial sensor that regulates bacterial phagosome functions in macrophages. *Nat Immunol*. 11:920-927.

Chang, L., and M. Karin. 2001. Mammalian MAP kinase signalling cascades. *Nature*. 410:37-40.

Chen, Q., D.W. Powell, M.J. Rane, S. Singh, W. Butt, J.B. Klein, and K.R. McLeish. 2003. Akt phosphorylates p47phox and mediates respiratory burst activity in human neutrophils. *J Immunol*. 170:5302-5308.

Clark, K., M. Peggie, L. Plater, R.J. Sorcek, E.R. Young, J.B. Madwed, J. Hough, E.G. McIver, and P. Cohen. 2011. Novel cross-talk within the IKK family controls innate immunity. *Biochem J*. 434:93-104.

Cocks, B.G., C.C. Chang, J.M. Carballido, H. Yssel, J.E. de Vries, and G. Aversa. 1995. A novel receptor involved in T-cell activation. *Nature*. 376:260-263.

Everts, B., E. Amiel, S.C. Huang, A.M. Smith, C.H. Chang, W.Y. Lam, V. Redmann, T.C. Freitas, J. Blagih, G.J. van der Windt, M.N. Artyomov, R.G. Jones, E.L. Pearce, and E.J. Pearce. 2014. TLR-driven early glycolytic reprogramming via the kinases TBK1-IKKvarepsilon supports the anabolic demands of dendritic cell activation. *Nat Immunol*. 15:323-332.

Farina, C., D. Theil, B. Semlinger, R. Hohlfeld, and E. Meinl. 2004. Distinct responses of monocytes to Toll-like receptor ligands and inflammatory cytokines. *Int Immunol*. 16:799-809.

Fitzgerald, K.A., S.M. McWhirter, K.L. Faia, D.C. Rowe, E. Latz, D.T. Golenbock, A.J. Coyle, S.M. Liao, and T. Maniatis. 2003a. IKKepsilon and TBK1 are essential components of the IRF3 signaling pathway. *Nat Immunol*. 4:491-496.

Fitzgerald, K.A., D.C. Rowe, B.J. Barnes, D.R. Caffrey, A. Visintin, E. Latz, B. Monks, P.M. Pitha, and D.T. Golenbock. 2003b. LPS-TLR4 signaling to IRF-3/7 and NF-kappaB involves the toll adapters TRAM and TRIF. *J Exp Med*. 198:1043-1055.

Fitzgerald, K.A., D.C. Rowe, and D.T. Golenbock. 2004. Endotoxin recognition and signal transduction by the TLR4/MD2-complex. *Microbes Infect*. 6:1361-1367.

Ford, E., and D. Thanos. 2010. The transcriptional code of human IFN-beta gene expression. *Biochim Biophys Acta*. 1799:328-336.

Gidon, A., S. Bardin, B. Cinquin, J. Boulanger, F. Waharte, L. Heliot, H. de la Salle, D. Hanau, C. Kervrann, B. Goud, and J. Salamero. 2012. A Rab11A/myosin Vb/Rab11-FIP2 complex frames two late recycling steps of langerin from the ERC to the plasma membrane. *Traffic*. 13:815-833.

Guichard, A., V. Nizet, and E. Bier. 2014. RAB11-mediated trafficking in host-pathogen interactions. *Nat Rev Microbiol*. 12:624-634.

Horgan, C.P., and M.W. McCaffrey. 2009. The dynamic Rab11-FIPs. *Biochem Soc Trans*. 37:1032-1036.

Hoyal, C.R., A. Gutierrez, B.M. Young, S.D. Catz, J.H. Lin, P.N. Tsichlis, and B.M. Babior. 2003. Modulation of p47PHOX activity by site-specific phosphorylation: Akt-dependent activation of the NADPH oxidase. *Proc Natl Acad Sci U S A*. 100:5130-5135.

Husebye, H., M.H. Aune, J. Stenvik, E. Samstad, F. Skjeldal, O. Halaas, N.J. Nilsen, H. Stenmark, E. Latz, E. Lien, T.E. Mollnes, O. Bakke, and T. Espevik. 2010. The Rab11a GTPase controls Toll-like receptor 4-induced activation of interferon regulatory factor-3 on phagosomes. *Immunity*. 33:583-596.

Husebye, H., O. Halaas, H. Stenmark, G. Tunheim, O. Sandanger, B. Bogen, A. Brech, E. Latz, and T. Espevik. 2006. Endocytic pathways regulate Toll-like receptor 4 signaling and link innate and adaptive immunity. *EMBO J*. 25:683-692.

Junutula, J.R., E. Schonteich, G.M. Wilson, A.A. Peden, R.H. Scheller, and R. Prekeris. 2004. Molecular characterization of Rab11 interactions with members of the family of Rab11-interacting proteins. *J Biol Chem*. 279:33430-33437.

Kagan, J.C., T. Su, T. Horng, A. Chow, S. Akira, and R. Medzhitov. 2008. TRAM couples endocytosis of Toll-like receptor 4 to the induction of interferon-beta. *Nat Immunol*. 9:361-368.

Kelly, B., and L.A. O'Neill. 2015. Metabolic reprogramming in macrophages and dendritic cells in innate immunity. *Cell Res*. 25:771-784.

Klein, D.C., A. Skjesol, E.D. Kers-Rebel, T. Sherstova, B. Sporsheim, K.W. Egeberg, B.T. Stokke, T. Espevik, and H. Husebye. 2015. CD14, TLR4 and TRAM Show Different Trafficking Dynamics During LPS Stimulation. *Traffic*. 16:677-690.

Krawczyk, C.M., T. Holowka, J. Sun, J. Blagih, E. Amiel, R.J. DeBerardinis, J.R. Cross, E. Jung, C.B. Thompson, R.G. Jones, and E.J. Pearce. 2010. Toll-like receptor-induced changes in glycolytic metabolism regulate dendritic cell activation. *Blood*. 115:4742-4749.

Laird, M.H., S.H. Rhee, D.J. Perkins, A.E. Medvedev, W. Piao, M.J. Fenton, and S.N. Vogel. 2009. TLR4/MyD88/PI3K interactions regulate TLR4 signaling. *J Leukoc Biol*. 85:966-977.

Lindsay, A.J., and M.W. McCaffrey. 2004. The C2 domains of the class I Rab11 family of interacting proteins target recycling vesicles to the plasma membrane. *J Cell Sci*. 117:4365-4375.

Ma, C., N. Wang, C. Detre, G. Wang, M. O'Keeffe, and C. Terhorst. 2012. Receptor signaling lymphocyte-activation molecule family 1 (Slamf1) regulates membrane fusion and NADPH oxidase 2 (NOX2) activity by recruiting a Beclin-1/Vps34/ultraviolet radiation resistance-associated gene (UVRAG) complex. *J Biol Chem*. 287:18359-18365.

Makani, S.S., K.Y. Jen, and P.W. Finn. 2008. New costimulatory families: signaling lymphocytic activation molecule in adaptive allergic responses. *Curr Mol Med*. 8:359-364.

Mancuso, G., A. Midiri, C. Biondo, C. Beninati, S. Zummo, R. Galbo, F. Tomasello, M. Gambuzza, G. Macri, A. Ruggeri, T. Leanderson, and G. Teti. 2007. Type I IFN signaling is crucial for host resistance against different species of pathogenic bacteria. *J Immunol*. 178:3126-3133.

Mikhalap, S.V., L.M. Shlapatska, A.G. Berdova, C.L. Law, E.A. Clark, and S.P. Sidorenko. 1999. CDw150 associates with src-homology 2-containing inositol phosphatase and modulates CD95-mediated apoptosis. *J Immunol*. 162:5719-5727.

Mogensen, T.H. 2009. Pathogen recognition and inflammatory signaling in innate immune defenses. *Clin Microbiol Rev*. 22:240-273, Table of Contents.

Oshiumi, H., M. Sasai, K. Shida, T. Fujita, M. Matsumoto, and T. Seya. 2003. TIR-containing adapter molecule (TICAM)-2, a bridging adapter recruiting to toll-like receptor 4 TICAM-1 that induces interferon-beta. *J Biol Chem*. 278:49751-49762.

Pfaffl, M.W. 2001. A new mathematical model for relative quantification in real-time RT-PCR. *Nucleic Acids Res*. 29:e45.

Poli-de-Figueiredo, L.F., A.G. Garrido, N. Nakagawa, and P. Sannomiya. 2008. Experimental models of sepsis and their clinical relevance. *Shock*. 30 Suppl 1:53-59.

Radtke, A.L., L.M. Delbridge, S. Balachandran, G.N. Barber, and M.X. O'Riordan. 2007. TBK1 protects vacuolar integrity during intracellular bacterial infection. *PLoS Pathog*. 3:e29.

Rethi, B., P. Gogolak, I. Szatmari, A. Veres, E. Erdos, L. Nagy, E. Rajnavolgyi, C. Terhorst, and A. Lanyi. 2006. SLAM/SLAM interactions inhibit CD40-induced production of inflammatory cytokines in monocyte-derived dendritic cells. *Blood*. 107:2821-2829.

Romanets-Korbut, O., A.M. Najakshin, M. Yurchenko, T.A. Malysheva, L. Kovalevska, L.M. Shlapatska, Y.A. Zozulya, A.V. Taranin, B. Horvat, and S.P. Sidorenko. 2015. Expression of CD150 in tumors of the central nervous system: identification of a novel isoform. *PLoS One*. 10:e0118302.

Romero, X., D. Benitez, S. March, R. Vilella, M. Miralpeix, and P. Engel. 2004. Differential expression of SAP and EAT-2-binding leukocyte cell-surface molecules CD84, CD150 (SLAM), CD229 (Ly9) and CD244 (2B4). *Tiss Antig*. 64:132-144.

Sakaguchi, S., H. Negishi, M. Asagiri, C. Nakajima, T. Mizutani, A. Takaoka, K. Honda, and T. Taniguchi. 2003. Essential role of IRF-3 in lipopolysaccharide-induced interferon-beta gene expression and endotoxin shock. *Biochem Biophys Res Commun*. 306:860-866.

Sanjana, N.E., O. Shalem, and F. Zhang. 2014. Improved vectors and genome-wide libraries for CRISPR screening. *Nat Methods*. 11:783-784.

Schindelin, J., I. Arganda-Carreras, E. Frise, V. Kaynig, M. Longair, T. Pietzsch, S. Preibisch, C. Rueden, S. Saalfeld, B. Schmid, J.Y. Tinevez, D.J. White, V. Hartenstein, K. Eliceiri, P. Tomancak, and A. Cardona. 2012. Fiji: an open-source platform for biological-image analysis. *Nat Methods*. 9:676-682.

Schroder, K., K.M. Irvine, M.S. Taylor, N.J. Bokil, K.A. Le Cao, K.A. Masterman, L.I. Labzin, C.A. Semple, R. Kapetanovic, L. Fairbairn, A. Akalin, G.J. Faulkner, J.K. Baillie, M. Gongora, C.O. Daub, H. Kawaji, G.J. McLachlan, N. Goldman, S.M. Grimmond, P. Carninci, H. Suzuki, Y. Hayashizaki, B. Lenhard, D.A. Hume, and M.J. Sweet. 2012. Conservation and divergence in Toll-like receptor 4-regulated gene expression in primary human versus mouse macrophages. *Proc Natl Acad Sci U S A*. 109:E944-953.

Shlapatska, L.M., S.V. Mikhalap, A.G. Berdova, O.M. Zelensky, T.J. Yun, K.E. Nichols, E.A. Clark, and S.P. Sidorenko. 2001. CD150 association with either the SH2-containing inositol phosphatase or the SH2-containing protein tyrosine phosphatase is regulated by the adaptor protein SH2D1A. *J Immunol*. 166:5480-5487.

Sidorenko, S.P., and E.A. Clark. 1993. Characterization of a cell surface glycoprotein IPO-3, expressed on activated human B and T lymphocytes. *J Immunol*. 151:4614-4624.

Theil, D., C. Farina, and E. Meinl. 2005. Differential expression of CD150 (SLAM) on monocytes and macrophages in chronic inflammatory contexts: abundant in Crohn's disease, but not in multiple sclerosis. *J Clin Pathol*. 58:110-111.

Thurston, T.L., K.B. Boyle, M. Allen, B.J. Ravenhill, M. Karpiyevich, S. Bloor, A. Kaul, J. Noad, A. Foeglein, S.A. Matthews, D. Komander, M. Bycroft, and F. Randow. 2016. Recruitment of TBK1 to cytosol-invading Salmonella induces WIPI2-dependent antibacterial autophagy. *EMBO J*. 35:1779-1792.

Toshchakov, V., B.W. Jones, P.Y. Perera, K. Thomas, M.J. Cody, S. Zhang, B.R. Williams, J. Major, T.A. Hamilton, M.J. Fenton, and S.N. Vogel. 2002. TLR4, but not TLR2, mediates IFN-beta-induced STAT1alpha/beta-dependent gene expression in macrophages. *Nat Immunol*. 3:392-398.

Trinchieri, G. 2010. Type I interferon: friend or foe? *J Exp Med*. 207:2053-2063.

Troutman, T.D., J.F. Bazan, and C. Pasare. 2012a. Toll-like receptors, signaling adapters and regulation of the pro-inflammatory response by PI3K. *Cell Cycle*. 11:3559-3567.

Troutman, T.D., W. Hu, S. Fulenchek, T. Yamazaki, T. Kurosaki, J.F. Bazan, and C. Pasare. 2012b. Role for B-cell adapter for PI3K (BCAP) as a signaling adapter linking Toll-like receptors (TLRs) to serine/threonine kinases PI3K/Akt. *Proc Natl Acad Sci U S A*. 109:273-278.

van Driel, B., G. Liao, X. Romero, M.S. O'Keeffe, G. Wang, W.A. Faubion, S.B. Berger, E.M. Magelky, M. Manocha, V. Azcutia, M. Grisham, F.W. Luscinskas, E. Mizoguchi, R. de Waal Malefyt, H.C. Reinecker, A.K. Bhan, N. Wang, and C. Terhorst. 2012. Signaling lymphocyte activation molecule regulates development of colitis in mice. *Gastroenterol*. 143:1544-1554 e1547.

van Driel, B.J., G. Liao, P. Engel, and C. Terhorst. 2016. Responses to Microbial Challenges by SLAMF Receptors. *Front Immunol*. 7:4.

Vaure, C., and Y. Liu. 2014. A comparative review of toll-like receptor 4 expression and functionality in different animal species. *Front Immunol*. 5:316.

Wang, N., A. Satoskar, W. Faubion, D. Howie, S. Okamoto, S. Feske, C. Gullo, K. Clarke, M.R. Sosa, A.H. Sharpe, and C. Terhorst. 2004. The cell surface receptor SLAM controls T cell and macrophage functions. *J Exp Med*. 199:1255-1264.

West, A.P., I.E. Brodsky, C. Rahner, D.K. Woo, H. Erdjument-Bromage, P. Tempst, M.C. Walsh, Y. Choi, G.S. Shadel, and S. Ghosh. 2011. TLR signalling augments macrophage bactericidal activity through mitochondrial ROS. *Nature*. 472:476-480.

Yamamoto, M., S. Sato, H. Hemmi, S. Uematsu, K. Hoshino, T. Kaisho, O. Takeuchi, K. Takeda, and S. Akira. 2003. TRAM is specifically involved in the Toll-like receptor 4-mediated MyD88-independent signaling pathway. *Nat Immunol*. 4:1144-1150.

Yamashiro, D.J., B. Tycko, S.R. Fluss, and F.R. Maxfield. 1984. Segregation of transferrin to a mildly acidic (pH 6.5) para-Golgi compartment in the recycling pathway. *Cell*. 37:789-800.

Figure legends

Figure 1. SLAMF1 is enriched in the Rab11-positive ERC in unstimulated macrophages, and SLAMF1 expression is induced by LPS and several other TLR ligands in primary human monocytes and macrophages. (A) Monocytes, macrophages and differentiated THP-1 cells stained with antibodies towards SLAMF1 (green) and GM130 (red) and imaged by confocal microscopy. (B) 3D-model of cis-Golgi (GM130) and SLAMF1 in THP-1 cells. Z-stacks from the GM130 and SLAMF1 channels were obtained using high-resolution confocal microscopy, followed by 3D-modeling in IMARIS software. (C) Macrophages stained for SLAMF1 and Rab11 (ERC marker), representative image. Overlapping pixels for SLAMF1 and Rab11 are shown in white overlay. tM1 = 0.683 ± 0.08 for z-stacks of ERC as region of interest (ROI), for 30 ROI analyzed per donor, where tM1 is Manders' co-localization coefficient with thresholds calculated in Coloc 2 Fiji plugin with anti-SLAMF1 staining as first channel, presented as mean with standard deviation (SD). (D) Macrophages co-stained for SLAMF1 and EEA1. (E) Macrophages co-stained for SLAMF1 and LAMP1. Co-localization accessed for Z-stacks for at least 30 cells for each experiment (4 total) showing no co-localization for both markers (D, E). (F) Flow cytometry analysis of SLAMF1 surface expression by primary macrophages and differentiated THP-1 cells. Cells co-stained for SLAMF1 and CD14, and gated for CD14-positive cells (primary cells), or stained for SLAMF1 (THP-1 cells). (G) Flow cytometry analysis of SLAMF1 surface expression by human macrophages stimulated by ultrapure K12 LPS (100 ng/ml) for 2, 4 and 6 h. (H) Western blot analysis of lysates from primary human macrophages stimulated by LPS for 2, 4 and 6 h. Graph present mean values for three biological replicates with SD (I, J) Quantification of *SLAMF1*mRNA expression by Q-PCR in monocytes (I) and macrophages (J) stimulated by TLRs' ligands FSL-1 (20 ng/ml), K12 LPS (100 ng/ml), CL075 (1 μg/ml) (I, J), and R848 (1 μg/ml), Pam3Cys (P3C, 1 μg/ml) or K12 *E. coli* particles (20/cell) (I). Results presented as mean with SD, statistical significance between groups evaluated by a two-tailed *t*-test, *significance level of $p < 0.01$ (I, J). Results are representative of at least 4 independent experiments/donors (A-H), or combined data for at least 3 donors (I, J).

Figure 2. Knockdown of SLAMF1 in macrophages results in the strongly reduced TLR4-mediated *IFNβ* mRNA expression and protein secretion, and some decrease of TNF, IL-6 and CXCL10 secretion. (A, B) Quantification of *SLAMF1*, *IFNβ* and *TNF* mRNA expression by Q-PCR in THP-1 cells (A) and macrophages (B) treated by 100 ng/ml ultrapure K12 LPS. (C, D) IFNβ and TNF secretion levels by THP-1 cells (C) and macrophages (D) in response to LPS (4 and 6 h) assessed by ELISA, secretion levels of IL-1β IL-6, IL-8 and CXCL-10 (6 h LPS) analyzed by Multiplex

assay (E, F). Data presented as mean with SD for combined data from three independent experiments for (A, C, E) or for three biological replicates from one of 6 donors (B, D) or one of 3 donors (F). Non-significant differences are marked by NS.

Figure 3. SLAMF1 silencing in macrophages impairs TLR4-mediated phosphorylation of TBK1, IRF3 and TAK1. Western blotting of lysates macrophages treated with a control non-silencing oligo or *SLAMF1*-specific siRNA oligo and stimulated with 100 ng/ml LPS. The antibodies used are indicated on the figure. Antibody towards SLAMF1 was used to control for SLAMF1 silencing, GAPDH was used as equal loading control. Graphs (right panels) show quantifications of protein levels relative to GAPDH levels obtained using Odyssey software. Western blots representative for one of five donors.

Figure 4. Lentiviral transduction of SLAMF1 in macrophages results in the increase of IRF3 and TBK1 phosphorylation in response to LPS and upregulation of IFNβ and TNF expression. (A) Quantification of *SLAMF1*, *IFNβ* and *TNF* mRNA expression of by Q-PCR in macrophages transduced by Flag-tagged SLAMF1-coding or control virus and treated by LPS. The Q-PCR data are presented as mean and SD for three biological replicates of one of three experiments, significance calculated by two-tailed *t*-test, $p < 0.01$. Non-significant differences marked by NS. (B) Western blots showing LPS-induced phosphorylation of signaling molecules in cells transduced with SLAMF1 expressing virus *vs.* control virus. Graphs (right panels) show quantifications of protein levels relative to GAPDH levels obtained with Odyssey software.

Figure 5. SLAMF1 regulates TRAM recruitment to *E. coli* phagosomes. (A) SLAMF1 co-staining with TRAM, EEA1 or LAMP1 in primary macrophages co-incubated with *E. coli* pHrodo particles for indicated time points. SLAMF1 (green), *E. coli* (blue) and TRAM, EEA1 or LAMP1 (red). The data shown are representative of one out of four donors. Scale bars represent 10 μm. B,C TRAM and SLAMF1 mean voxel intensities (MIs) on *E. coli* phagosomes upon SLAMF1 silencing (B) or simultaneous Rab11a and Rab11b silencing (C) in primary human macrophages, quantified from xyz images. The scatter plots are presented as median values of TRAM voxel intensity, and *n*= number of phagosomes. The nonparametric Mann-Whitney test was used to evaluate statistical significance. *** $p < 0.0001$, *$p \leq 0.01$. Human macrophages were incubated with *E. coli* particles for indicated time points, fixed and co-stained for SLAMF1 and TRAM, normal rabbit (rIgG) or mouse IgG (mIgG). The data shown are representative for one out of 5 (B) or 4 (C) donors.

Figure 6. SLAMF1 interacts with TRAM protein. (A) Endogenous IPs using specific anti-SLAMF1 mAbs from macrophages stimulated by LPS. (B) Endogenous IPs using anti-TRAM pAbs from macrophages stimulated by LPS. (C) $TRAM^{Flag}$ precipitated SLAMF1, and SLAMF1 cytoplasmic tail (ct) was needed for interaction with TRAM. (D) Co-precipitation of TRAM deletion mutants – TIR domain (68-235), short TRAM TIR domain (68-176 aa), N-terminal (1-68 aa) or C-terminal (158-235 aa) domains with SLAMF1 protein. (E) Co-precipitation of TRAM deletion mutants containing N-terminal part of TRAM TIR domain with SLAMF1. (F) Co-precipitation of $SLAMF1^{Flag}$ deletion mutants with $TRAM^{YFP}$. (G) Co-precipitation of human $SLAMF1^{Flag}$ with human $TRAM^{YFP}$ and of mouse $SLAMF1^{Flag}$ with mouse $TRAM^{EGFP}$. (H) Human SLAMF1ct co-precipitation with $TRAM^{YFP}$ with or without amino acid substitutions (321-324). Graphs under figures (C-F) summarize IPs' results. Indicated constructs were transfected to HEK 293T cells, anti-Flag agarose was used for the IPs. For endogenous IPs a specific SLAMF1 or TRAM antibodies were covalently coupled to beads. At least three independent experiments were carried out for anti-Flag IPs, five independent experiments carried out for the endogenous IPs, one representative experiment shown for each.

Figure 7. SLAMF1 interacts with all class I Rab11 FIPs. (A) Anti-Flag IPs for $Rab11a^{Flag}$ with EGFP-tagged Rab11FIPs (1-5) and SLAMF1. (B) Schematic figure for class I and class II Rab11 FIPs domain structure. C2 - phospholipid-binding C2-domain, RBD - Rab11 binding domain, PRR - proline-rich region, EF - EF-hand domain. (C) Homologous protein sequence in class I FIPs, which follows C2 domain. Identical aa in all three class I FIPs are highlighted. (D) Co-precipitation of $SLAMF1^{Flag}$ with $FIP2^{EGFP}$ WT or FIP2 deletion mutant lacking C2 domain (ΔC2). (E, F) Co-precipitation of untagged SLAMF1 with $Rab11FIP2^{Flag}$ (1-512 aa) and Flag-tagged FIP2 deletion mutants in anti-Flag IPs in the absence (E) or presence (F) of overexpressed $Rab11^{CFP}$. (G) Quantification of co-precipitations (E, F) between SLAMF1 and $FIP2^{Flag}$ variants correlated to the amount of Flag-tagged protein on the blot and Flag-tagged protein sizes. Bars represent mean ± SD for three independent experiments. (H) Co-precipitation of $Rab11FIP2^{Flag}$ with SLAMF1 and Rab11a WT, or Rab11a Q70L mutant, or Rab11a S25N mutant. (I) Co-precipitation of $SLAMF1^{Flag}$ deletion mutants with $FIP2^{EGFP}$. (J) Scheme for FIP2 and TRAM interacting domains in SLAMF1ct. The results are representative for at least 3 independent experiments.

Figure 8. TRAM acts as a bridge between SLAMF1 and TLR4 signaling complex. (A, B) Co-precipitations of $SLAMF1^{Flag}$ with $TLR4^{Cherry}$ (A) or $TRIF^{HA}$ (B) with or without $TRAM^{YFP}$ overexpression. (C) Co-precipitation of $TLR4^{Flag}$ with SLAMF1 with or without $TRAM^{YFP}$ overexpression. (D) $TLR4^{Flag}$ interaction with $TRAM^{YFP}$ and $TRIF^{HA}$ with or without SLAMF1 co-

expression. (E) Co-precipitation of SLAMF1 with or without $TRIF^{HA}$ in the presence of $TRAM^{YFP}$ by $TLR4^{Flag}$. Indicated constructs were transfected to HEK 293T cells. pDuo-CD14/MD-2 vector was co-transfected to all wells (A, C-E). Anti-Flag agarose was used for IPs. At least three independent experiments were performed.

Figure 9. TRAM and SLAMF1 are essential for killing of *E. coli* by human macrophages. (A) Flow cytometry analysis of dihydrorhodamine 123 (DHR-123) fluorescence to access ROS activation in control siRNA or *SLAMF1* siRNA human macrophages upon stimulation by *E. coli* red pHrodo particles, one of 3 experiments shown. (A, B) Bacterial killing assays by SLAMF1 silenced and control THP-1 cells (B) and TRAM KO and control THP-1 cells (C) infected with DH5α strain at MOI 40. (D, E) Western blot analysis of pAkt (S473) and pIRF3 (S396) levels induced by *E. coli* particles in THP-1wt and TRAM KO cells (D) and SLAMF1 silenced or control oligo treated cells (E). Graphs (right panels) on Western blotting (D, E) show quantification of protein levels relative to β-tubulin, obtained with Odyssey software. (F) Western blot showing phospho-(S396) IRF3 and phospho- (S473) Akt levels in lysates of THP-1 cells co-incubated with *E. coli* particles for 1 hr in the presence or absence of TBK1-IKKε inhibitor (MRT67307), pan-Akt allosteric inhibitor (MK2206) or DMSO. (G) Bacterial killing assays by THP-1 cells with DMSO (< 0.01%), 1 μM Akt inhibitor MK2206, or 2 μM TBK1-IKKε inhibitor MRT67307 upon infection by DH5α at MOI 40. Percent killing (B, C, G) was calculated = 100 - [(#CFU at time X / #CFU at time 0) x 100] for average values of technical replicates, each dot on the graphs (B, C, G) represents a biological replicate from 3 independent experiments, median value shown by line. Statistical significance calculated by Mann-Whitney non-parametric test, *** $p < 0.001$, ** $p < 0.01$.

Table 1. Primers used for cloning of full size or deletion mutants of SLAMF1, TRAM, TLR4 and Rab11 FIP2.

Construct		Primer sequence	Restriction enzyme	PCR product, mapped on nucleotide sequence
SLAMF1 (NM_003037.3)				
pcDNA3.1 and pLVX-EF1α-IRES-ZsGreen1	**For**	TTCGAATTCTGATGGGATCCCAAGGGGCTCC	**EcoRI**	
	Rev	GCAGCGGCCGCTCAGCTCTCTGGAAGTGTCA	**NotI**	**367-1374**
C-terminal DYKDDDDK	**For**	TTAGAATTCATGGATCCCAAGGGGCTCC	**EcoRI**	
	Rev	GGTACCTCGAGAGCTCTCTGGAAGTGTCACAC	**XhoI**	**367-1371**
pGEX-2TK	**For**	TATGGATCCCAGTTGAGAAGAAGAGGTAAAACG	**BamHI**	
	Rev	ATAGAATTCTCAGCTCTCTGGAAGTGTCAC	**EcoRI**	**1141-1374**
SLAMF1 (NM_003037.3) deletion mutants to C-terminal DYKDDDDK				
All deletion mutants	**For**	TTAGAATTCATGGATCCCAAGGGGCTCC	**EcoRI**	**-**
1-265 a.a	**Rev**	GGTACCTCGAGATTTACCTCTTCTTCTCAACTGTAG	**XhoI**	**367-1161**
1-326 a.a	**Rev**	GTACCTCGAGAGACTGTGATGGAATTTGTTTCCTG	**XhoI**	**367-1344**
1-330 a.a	**Rev**	GTACCTCGAGACACACTAGCATAGACTGTGATG	**XhoI**	**367-1356**
SLAMF1 (NM_003037.3) deletion mutant to pcDNA3.1				
	For	TTCGAATTCTGATGGGATCCCAAGGGGCTCC	**EcoRI**	
1-265 aa	**Rev**	TTAAGCGGCCGCTCATTTACCTCTTCTTCTCAACTG	**NotI**	**367-1161**
SLAMF1 (NM_003037.3) mutants with amino acid substitutions to C-terminal DYKDDDDK				
SLAMF1 Y281F	**For**	TTAGAATTCATGGATCCCAAGGGGCTCC	**EcoRI**	**367-1225**
	Rev	GTTTCTGGACTTGGGCAAAGATCGTAAGGC		
	For	GCCTTACGATCTTTGCCCAAGTCCAGAAAC		**1196-1371**
	Rev	GGTACCTCGAGATTTACCTCTTCTTCTCAACTGTAG	**XhoI**	
SLAMF1 Y327F	**For**	TTAGAATTCATGGATCCCAAGGGGCTCC	**EcoRI**	**367-1371**
	Rev	GGTACCTCGAGAGCTCTCTGGAAGTGTCACACTAGCAAA G ACTGTG	**XhoI**	
SLAMF1 TNSI/PNPT	**For**	TTAGAATTCATGGATCCCAAGGGGCTCC	**EcoRI**	**367-1341**
	Rev	TGTGGTGGGGTTTGGTTCCTGGACAGACTCTGG		
	For	GAACCAAACCCCACCACAGTCTATGCTAGTGTGACACTT C		**1324-1371 (plus vector)**
	Rev	CTTGTCATCGTCGTCCTTG (on C-terminal DYKDDDDK vector)		
TRAM/TICAM-2 (NM_021649.7)				
C-terminal DYKDDDDK	**For**	CATGAATTCATGGGTATCGGGAAGTCTAAA	**EcoRI**	
	Rev	TTAACTCGAGCGGCAATAAATTGTCTTTGTACC	**XhoI**	**443-1147**
TRAM deletion mutants to C-terminal DYKDDDDK				
1-68	**For**	CATGAATTCATGGGTATCGGGAAGTCTAAA	**EcoRI**	
	Rev	TTAACTCGAGCCATCTCTTCCACGCTCTGAGC	**XhoI**	**443-646**
1-79	**For**	CATGAATTCATGGGTATCGGGAAGTCTAAA	**EcoRI**	
	Rev	TTACCTCGAGAGAGGAACACCTCTTCTTCAGC	**XhoI**	**443-679**
1-90	**For**	CATGAATTCATGGGTATCGGGAAGTCTAAA	**EcoRI**	
	Rev	TTACCTCGAGATGTGTCATCTTCTGCATGCAATATC	**XhoI**	**443-712**
1-100	**For**	CATGAATTCATGGGTATCGGGAAGTCTAAA	**EcoRI**	
	Rev	TTACCTCGAGATAGCAGATTCTGGACTCTGAGG	**XhoI**	**443-742**
1-120	**For**	CATGAATTCATGGGTATCGGGAAGTCTAAA	**EcoRI**	
	Rev	TTACCTCGAGACTGTCTGCCACATGGCATCTC	**XhoI**	**443-802**
68-235	**For**	CATGAATTCATGTTTGAAGAAGAAGCTGAA	**EcoRI**	
	Rev	TTAACTCGAGCGGCAATAAATTGTCTTTGTACC	**XhoI**	**644-1147**
68-176	**For**	CATGAATTCATGTTTGAAGAAGAAGCTGAA	**EcoRI**	
	Rev	TTAACTCGAGCCAGGGGCCGCATGGGTATAACAG	**XhoI**	**644-970**

	For	CATGAATTCATGAACTCCGTTAACAGGCAGC	**EcoRI**	
158-235 aa	**Rev**	TTAACTCGAGCGGCAATAAATTGTCTTTGTACC	**XhoI**	**914-1147**
TLR4 (NM_138554.4)				
	For	CGGTCGACCGAGATCTCATGATGTCTGCCTCGCGCCTGG	**-**	
C-terminal DYKDDDDK	**Rev**	CTTGTAGTCGCCGGTACCGATAGATGTTGCTTCCTGCCA ATTG	**-**	**299-2815**
Mus Musculus TRAM/Ticam-2 (NM_173394.3) to EGFP-N1				
1-232 aa	**For**	ACTAAGCTTATGGGTGTTGGGAAGTCTAAAC	**HindIII**	**477-1175**
	Rev	ATATGGATCCCGGGCAATGAACTGTTTCTGCGAC	**BamHI**	
Mus Musculus Slamf1 (NM_013730.4) from pDisplay vector to C-terminal DYKDDDDK				
30-343 aa	**For**	TTGGAATTCGGCTTGGGGATATCCACCATGG	**EcoRI**	**183-1127**
	Rev	TATACCTCGAGAGCTCTCTGGCAGTGTCACACTG	**XhoI**	
Rab11 FIP2 (NM_014904.2) and deletion mutants to N-terminal DYKDDDDK				
All constructs	**For**	GCCCGAATTCGGCTGTCCGAGCAAGCCCAAAAG	**EcoRI**	
1-512 aa	**Rev**	ATAGCGGCCGCTCATTAACTGTTAGAGAATTTGCCAGC	**NotI**	**446-1980**
1-327 aa	**Rev**	ATAGCGGCCGCTCATTCGCTGCTTTCTTCAAATGG	**NotI**	**446-1429**
1-290 aa	**Rev**	ATAGCGGCCGCTTACACAATGCTGTCAGGTTGG	**NotI**	**446-1310**
1-254 aa	**Rev**	ATAGCGGCCGCTTATCCGAGAAGATGTGTTTGACC	**NotI**	**446-1199**
1-192 aa	**Rev**	ATAGCGGCCGCTTAGTGAGTACTTGGAATGATTGC	**NotI**	**446-1016**
Rab11a (NM_004663.4) QL and SN mutants to pECFP-C1				
1-216 aa	**For**	ATCAGTCGACATGGGCACCCGCGACGAC	**SalI**	**128-145**
	Rev	TTAAGGATCCTTATATGTTCTGACAGCACTG	**BamHI**	**758-774**

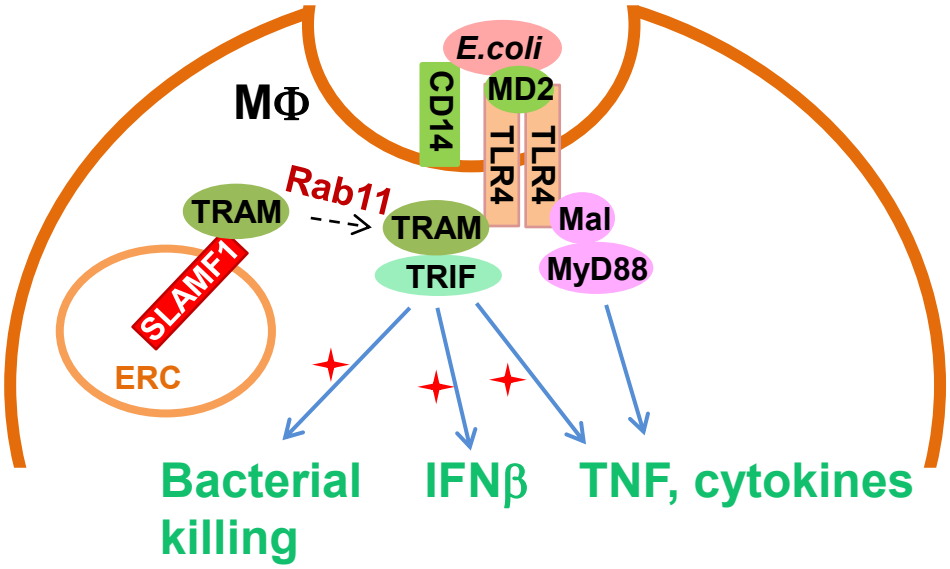

Graphical abstract

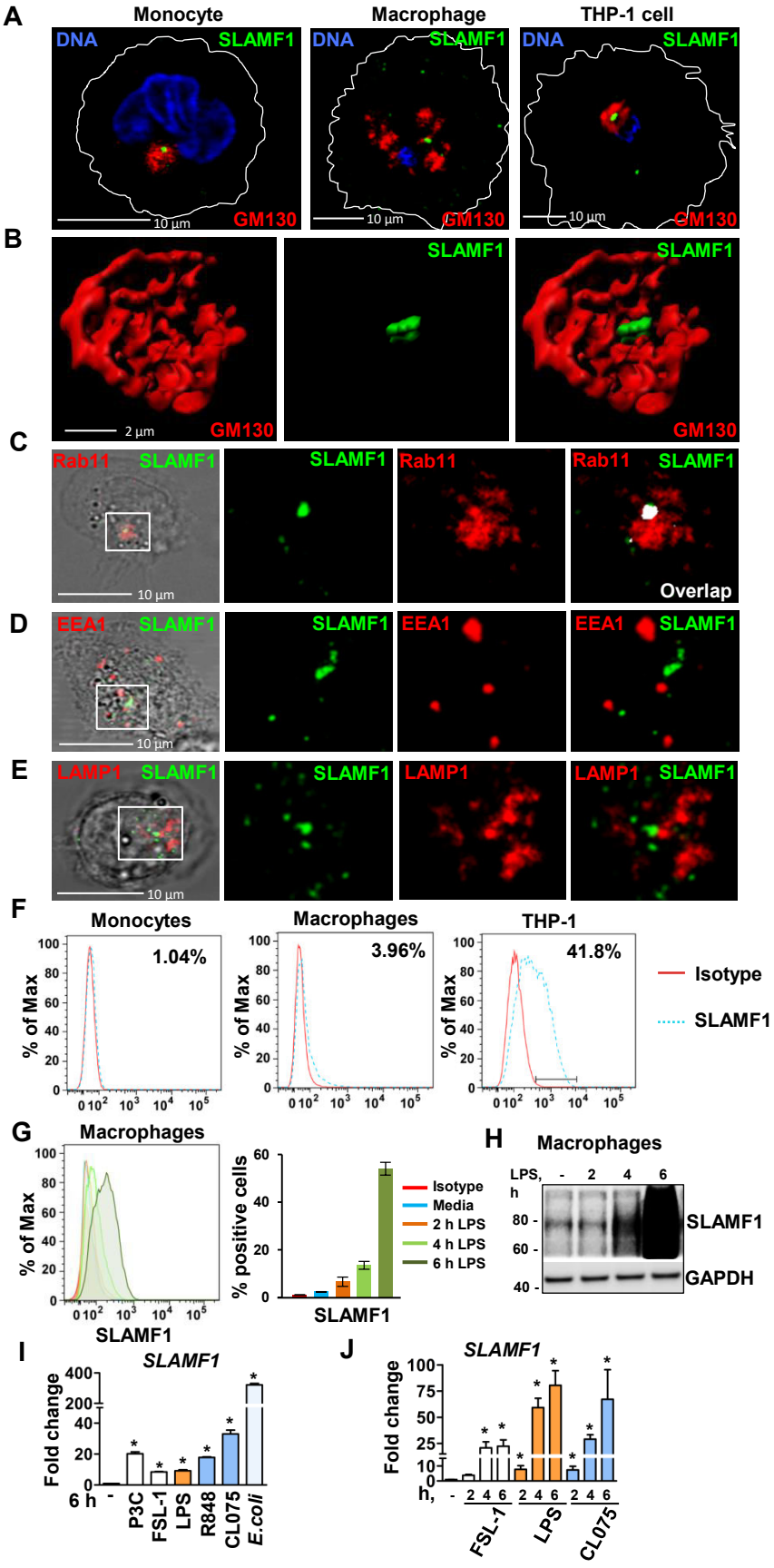
A
Monocyte
Macrophage
THP-1 cell
DNA
SLAMF1
GM130
10 µm
B
2 µm
C
Rab11
SLAMF1
Overlap
D
EEA1
E
LAMP1
F
Monocytes
Macrophages
THP-1
1.04%
3.96%
41.8%
% of Max
Isotype
SLAMF1
G
Macrophages
% positive cells
Isotype
Media
2 h LPS
4 h LPS
6 h LPS
H
Macrophages
LPS, h
- 2 4 6
80 -
60 -
40 -
SLAMF1
GAPDH
I
SLAMF1
Fold change
6 h
-
P3C
FSL-1
LPS
R848
CL075
E.coli
J
SLAMF1
Fold change
h, - 2 4 6 2 4 6 2 4 6
FSL-1
LPS
CL075

Figure 1

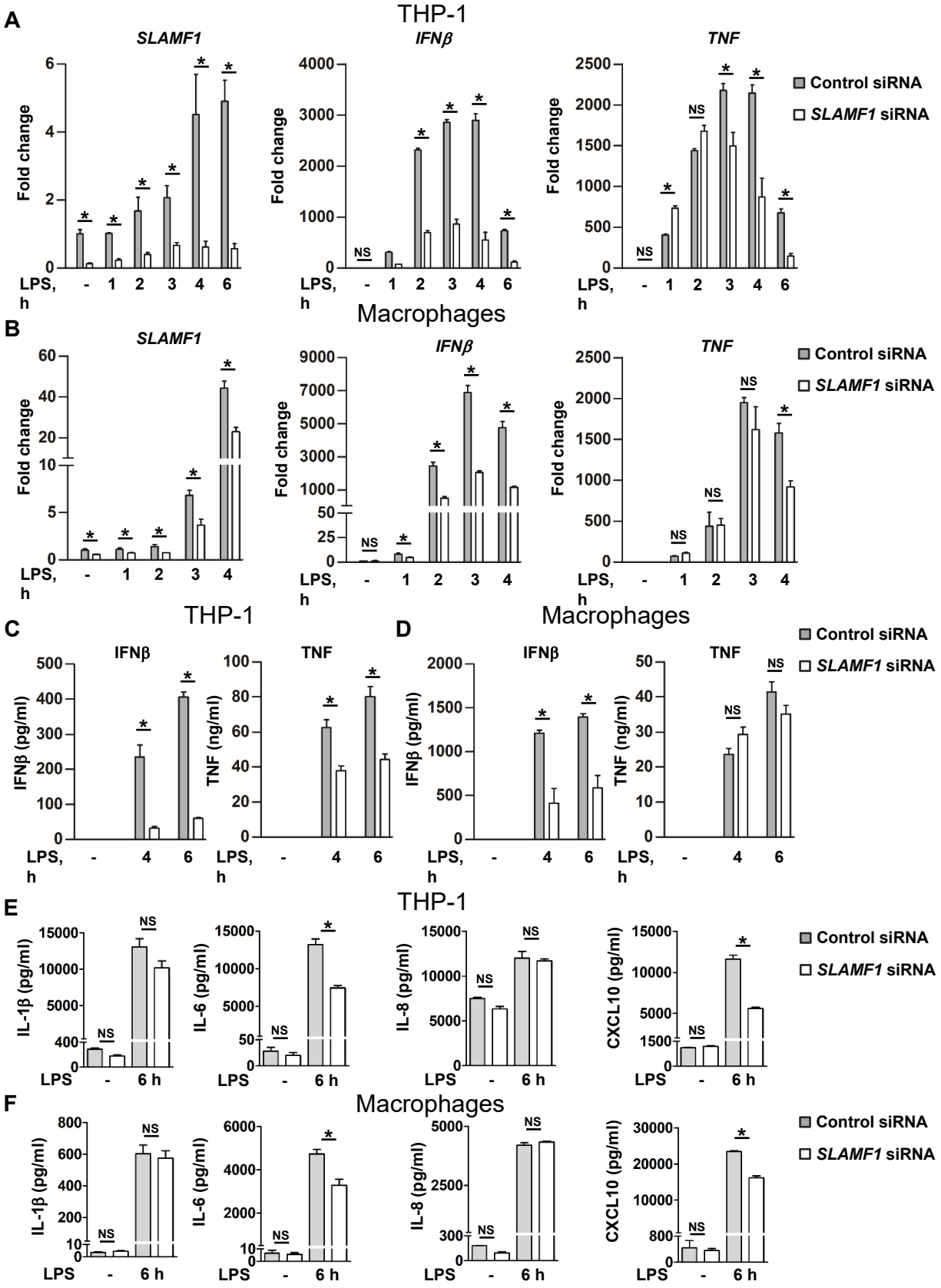
A
THP-1
SLAMF1
IFNβ
TNF
Fold change
LPS, h
Control siRNA
SLAMF1 siRNA
B
Macrophages
C
IFNβ (pg/ml)
TNF (ng/ml)
D
E
IL-1β (pg/ml)
IL-6 (pg/ml)
IL-8 (pg/ml)
CXCL10 (pg/ml)
LPS
6 h
F
NS

Figure 2

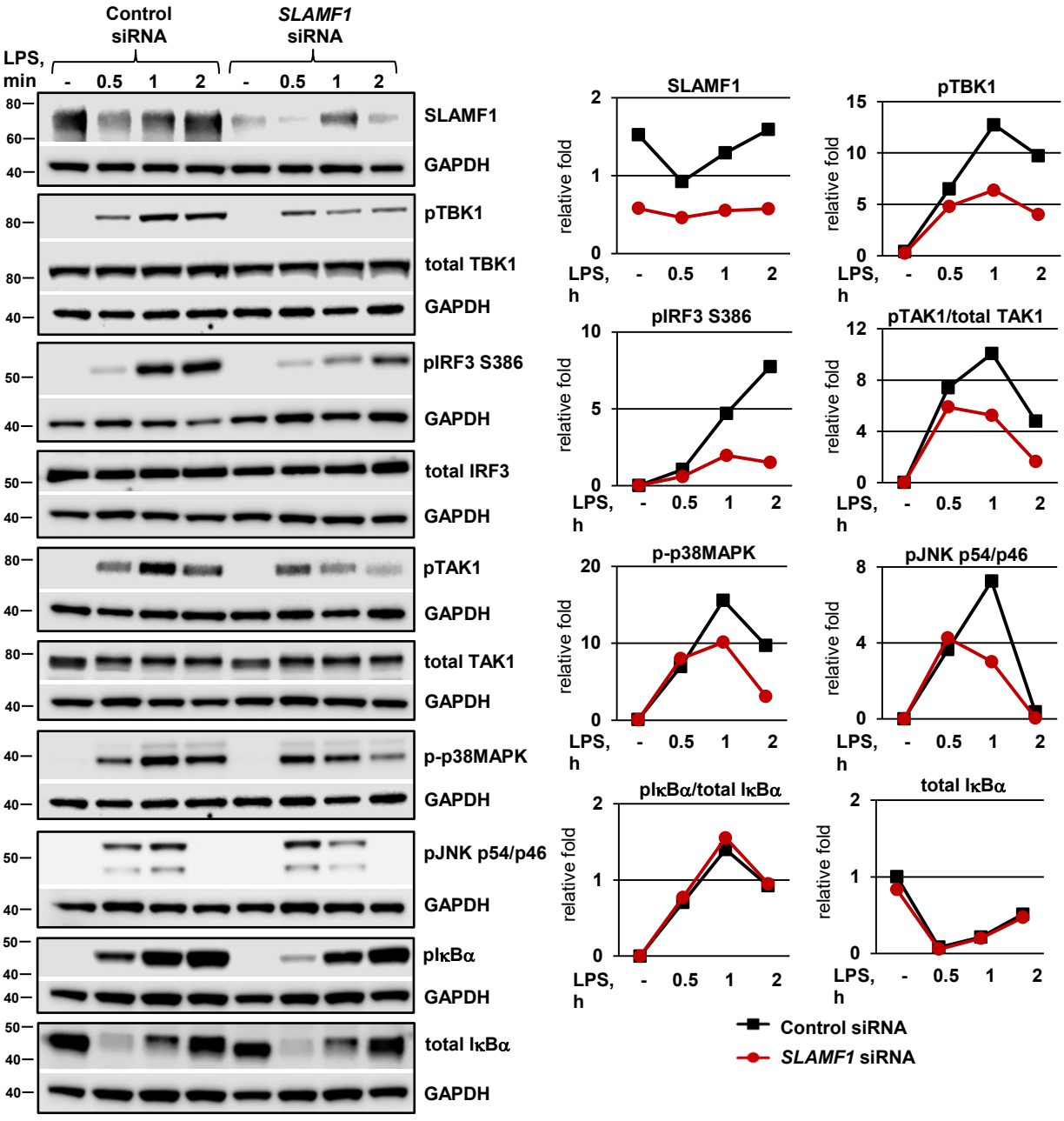
Control siRNA
SLAMF1 siRNA
LPS, min
- 0.5 1 2 - 0.5 1 2
SLAMF1
GAPDH
pTBK1
total TBK1
pIRF3 S386
total IRF3
pTAK1
total TAK1
p-p38MAPK
pJNK p54/p46
pIκBα
total IκBα
relative fold
LPS, h
pTAK1/total TAK1
pIκBα/total IκBα
Control siRNA
SLAMF1 siRNA

Figure 3

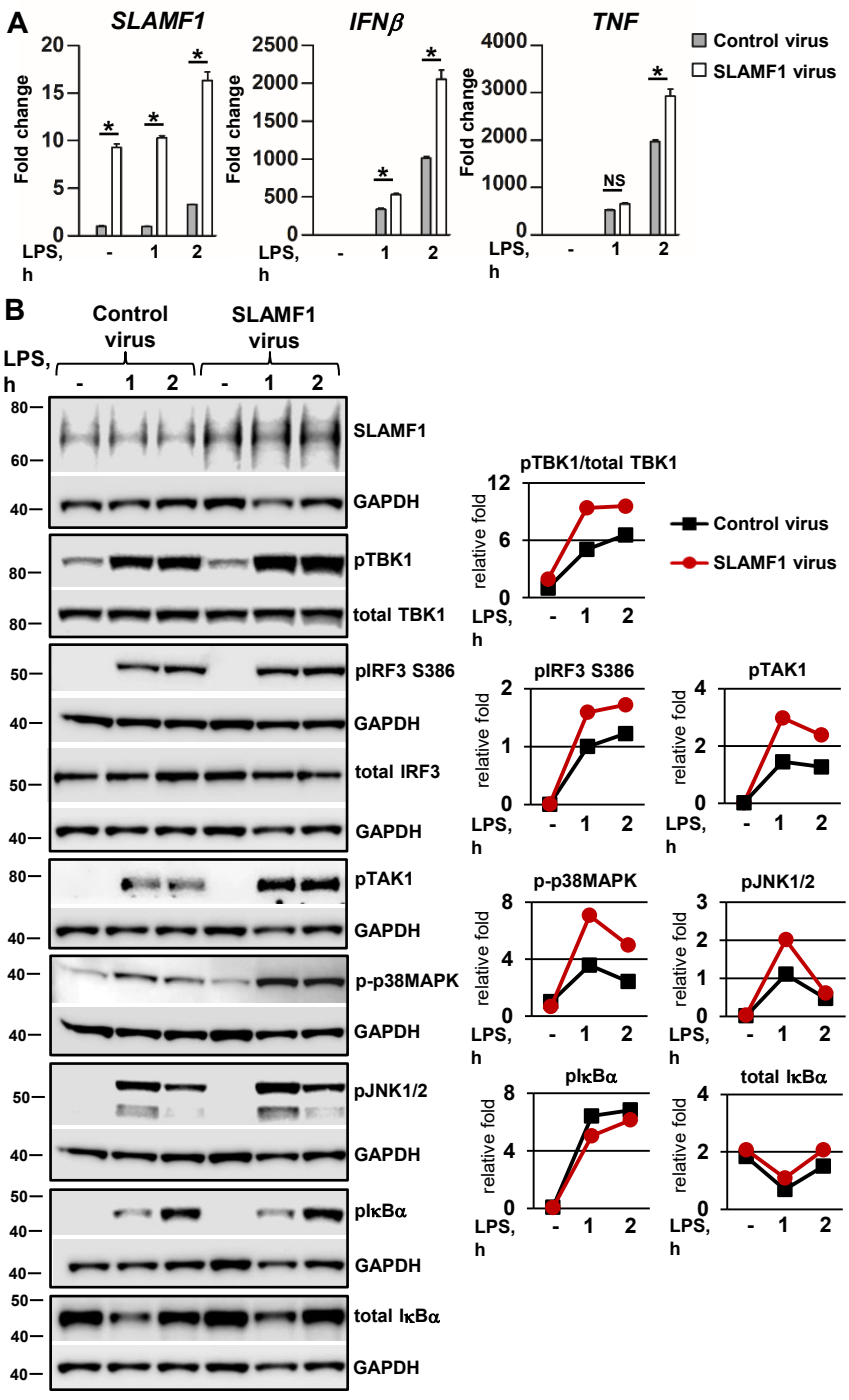
A
SLAMF1
IFNβ
TNF
Fold change
Control virus
SLAMF1 virus
LPS, h
NS
B
Control virus
SLAMF1 virus
LPS, h
SLAMF1
GAPDH
pTBK1
total TBK1
pIRF3 S386
total IRF3
pTAK1
p-p38MAPK
pJNK1/2
pIκBα
total IκBα
pTBK1/total TBK1
relative fold
pTAK1
p-p38MAPK
pJNK1/2
pIκBα
total IκBα

Figure 4

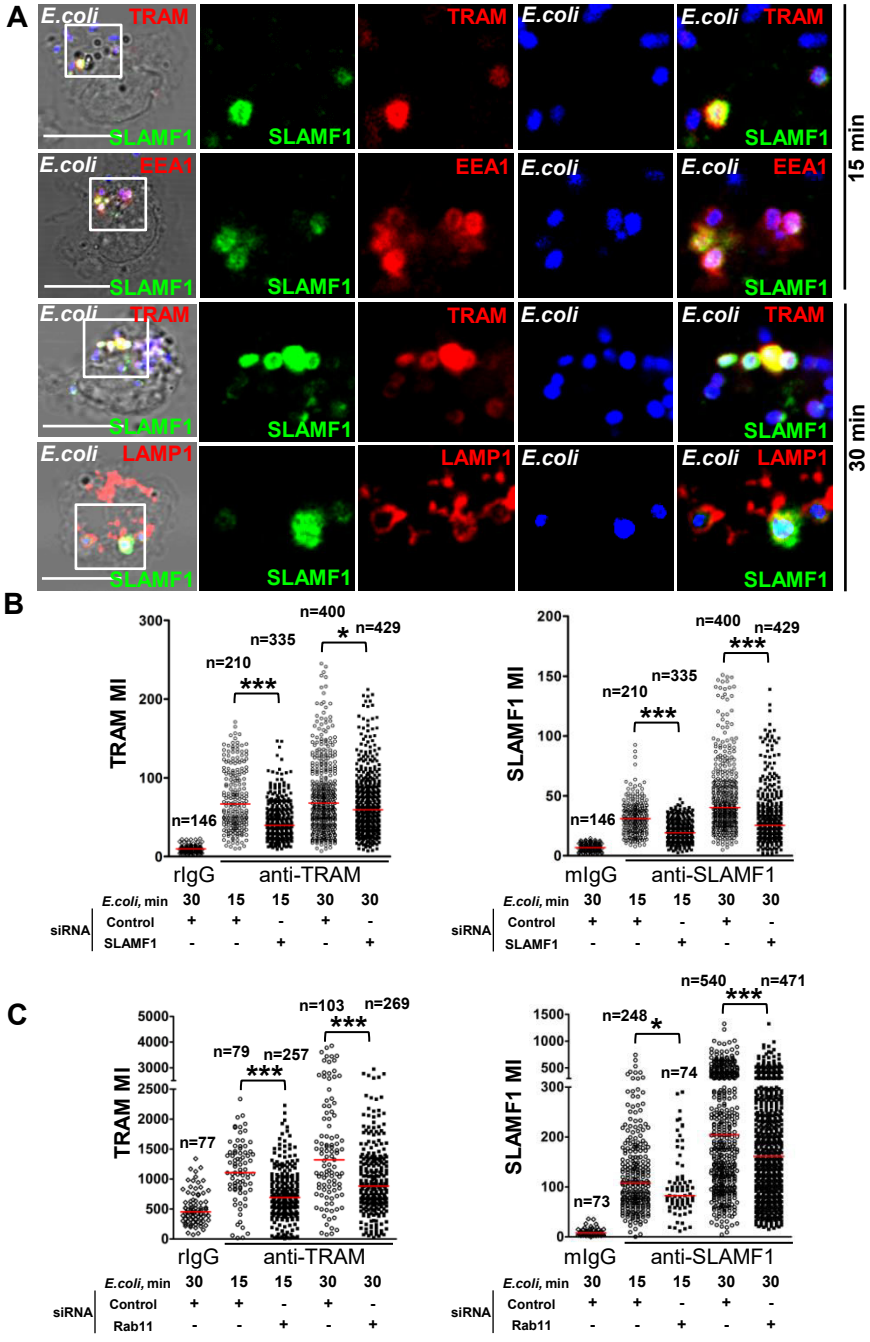
A
E.coli TRAM SLAMF1
TRAM SLAMF1
E.coli
E.coli TRAM SLAMF1
15 min
E.coli EEA1 SLAMF1
EEA1 SLAMF1
E.coli
E.coli EEA1 SLAMF1
E.coli TRAM SLAMF1
TRAM SLAMF1
E.coli
E.coli TRAM SLAMF1
30 min
E.coli LAMP1 SLAMF1
LAMP1 SLAMF1
E.coli
E.coli LAMP1 SLAMF1
B
TRAM MI
n=146
n=210
n=335
n=400
n=429
***
*
rIgG
anti-TRAM
SLAMF1 MI
mIgG
anti-SLAMF1
E.coli, min 30 15 15 30 30
siRNA Control + + - + -
SLAMF1 - - + - +
C
TRAM MI
n=77
n=79
n=257
n=103
n=269
rIgG
anti-TRAM
SLAMF1 MI
n=73
n=248
n=74
n=540
n=471
mIgG
anti-SLAMF1
E.coli, min 30 15 15 30 30
siRNA Control + + - + -
Rab11 - - + - +

Figure 5

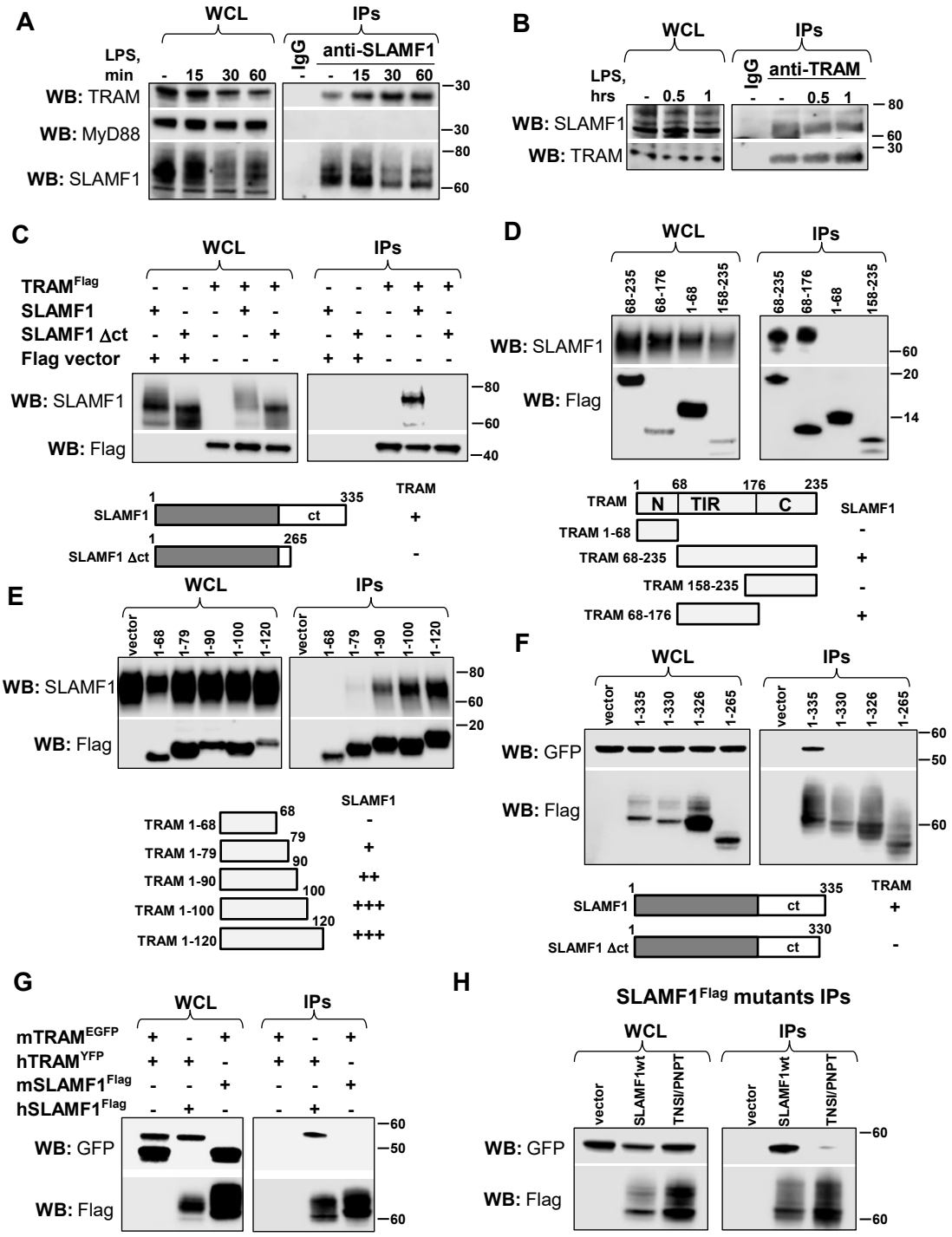
A
WCL
IPs
LPS, min
- 15 30 60
IgG
anti-SLAMF1
- 15 30 60
WB: TRAM
WB: MyD88
WB: SLAMF1
30
30
80
60
B
WCL
IPs
LPS, hrs
- 0.5 1
IgG
anti-TRAM
- - 0.5 1
WB: SLAMF1
WB: TRAM
80
60
30
C
WCL
IPs
TRAMFlag
SLAMF1
SLAMF1 Δct
Flag vector
WB: SLAMF1
WB: Flag
80
60
40
SLAMF1
1
335
ct
SLAMF1 Δct
265
TRAM
+
-
D
WCL
IPs
68-235
68-176
1-68
158-235
WB: SLAMF1
WB: Flag
60
20
14
TRAM
1
68
176
235
N
TIR
C
SLAMF1
TRAM 1-68
TRAM 68-235
TRAM 158-235
TRAM 68-176
E
WCL
IPs
vector
1-68
1-79
1-90
1-100
1-120
WB: SLAMF1
WB: Flag
80
60
20
SLAMF1
TRAM 1-68
68
TRAM 1-79
79
TRAM 1-90
90
TRAM 1-100
100
TRAM 1-120
120
-
+
++
+++
+++
F
WCL
IPs
vector
1-335
1-330
1-326
1-265
WB: GFP
WB: Flag
60
50
60
SLAMF1
1
335
ct
TRAM
+
SLAMF1 Δct
330
-
G
WCL
IPs
mTRAMEGFP
hTRAMYFP
mSLAMF1Flag
hSLAMF1Flag
WB: GFP
WB: Flag
60
50
60
H
SLAMF1Flag mutants IPs
WCL
IPs
vector
SLAMF1wt
TNSI/PNPT
WB: GFP
WB: Flag
60
60

Figure 6

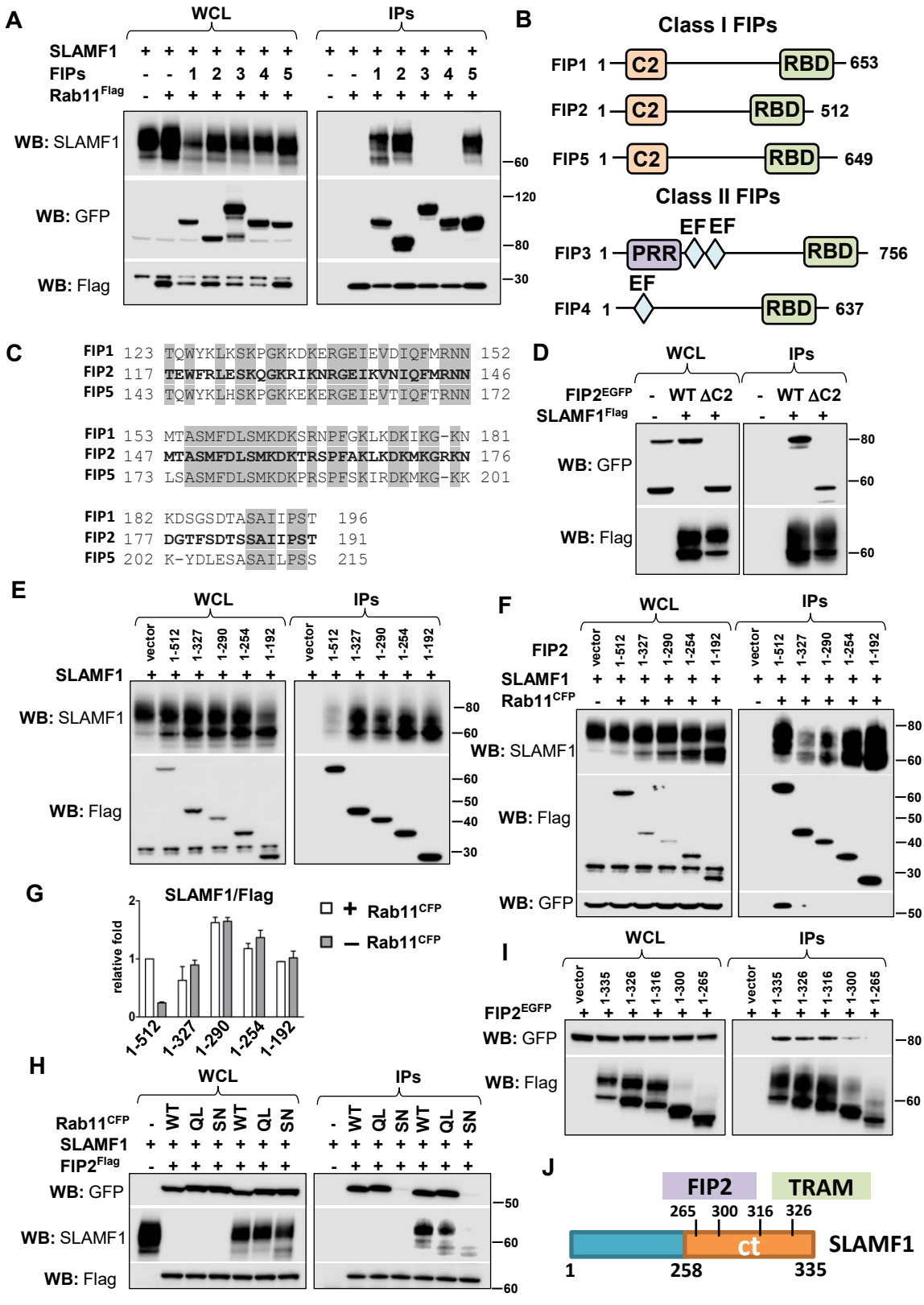
A
WCL
IPs
SLAMF1
FIPs
Rab11Flag
WB: SLAMF1
WB: GFP
WB: Flag
B
Class I FIPs
FIP1 1 C2 RBD 653
FIP2 1 C2 RBD 512
FIP5 1 C2 RBD 649
Class II FIPs
EF EF
FIP3 1 PRR RBD 756
EF
FIP4 1 RBD 637
C
FIP1 123 TQWYKLKSKPGKKDKERGEIEVDIQFMRNN 152
FIP2 117 TEWFRLESKQGKRIKNRGEIKVNIQFMRNN 146
FIP5 143 TQWYKLHSKPGKKEKERGEIEVTIQFTRNN 172
FIP1 153 MTASMFDLSMKDKSRNPFGKLKDKIKG-KN 181
FIP2 147 MTASMFDLSMKDKTRSPFAKLKDKMKGRKN 176
FIP5 173 LSASMFDLSMKDKPRSPFSKIRDKMKG-KK 201
FIP1 182 KDSGSDTASAIIPST 196
FIP2 177 DGTFSDTSSAIIPST 191
FIP5 202 K-YDLESASAILPSS 215
D
FIP2EGFP
SLAMF1Flag
WT ΔC2
E
vector
1-512
1-327
1-290
1-254
1-192
F
FIP2
Rab11CFP
G
SLAMF1/Flag
relative fold
+ Rab11CFP
— Rab11CFP
H
Rab11CFP
FIP2Flag
WT
QL
SN
I
1-335
1-326
1-316
1-300
1-265
J
FIP2
TRAM
265
300
316
326
ct
SLAMF1
1
258
335

Figure 7

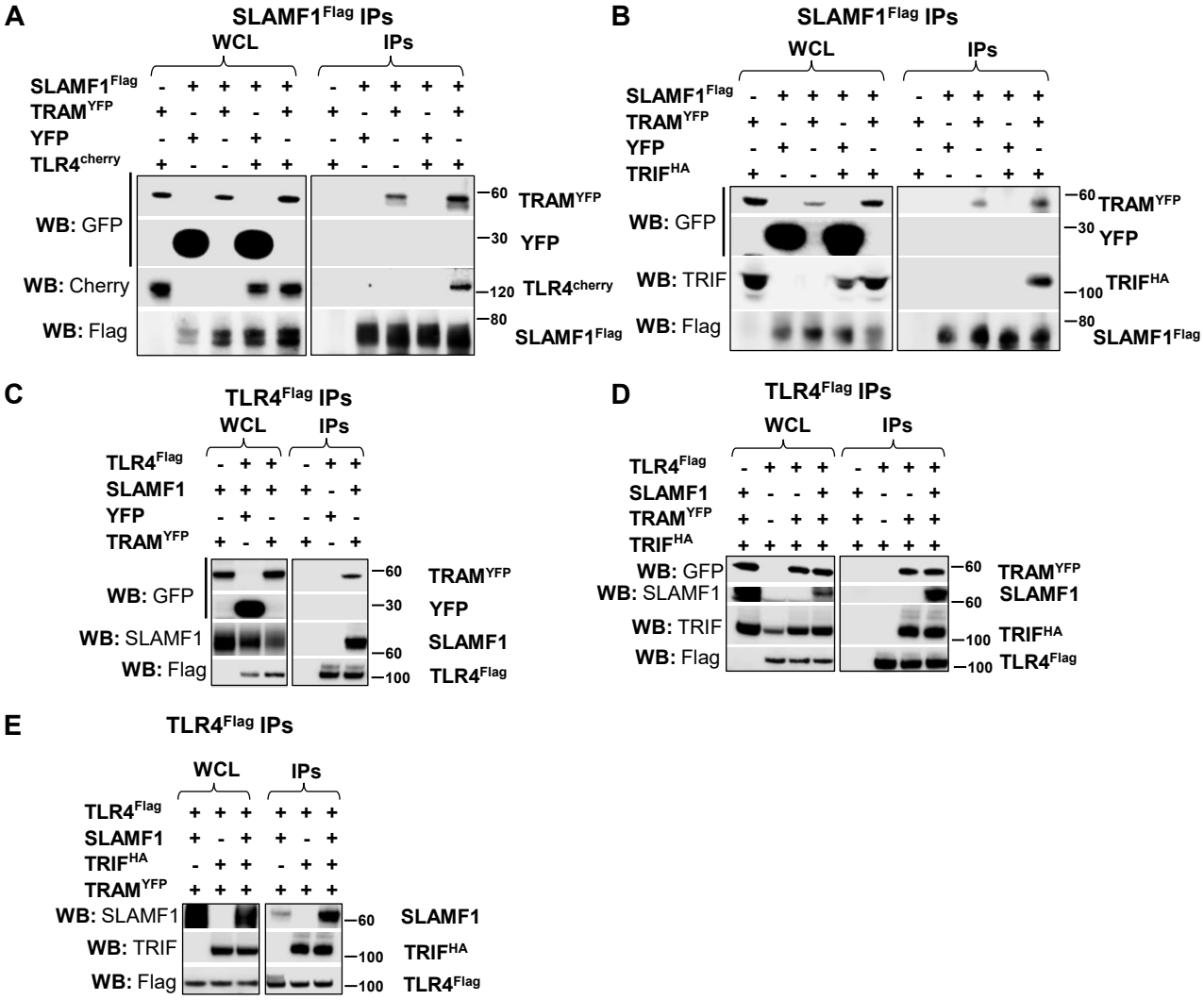
A
SLAMF1Flag IPs
WCL
IPs
SLAMF1Flag
TRAMYFP
YFP
TLR4cherry
WB: GFP
WB: Cherry
WB: Flag
60
30
120
80
TRAMYFP
YFP
TLR4cherry
SLAMF1Flag
B
SLAMF1Flag IPs
WCL
IPs
SLAMF1Flag
TRAMYFP
YFP
TRIFHA
WB: GFP
WB: TRIF
WB: Flag
60
30
100
80
TRAMYFP
YFP
TRIFHA
SLAMF1Flag
C
TLR4Flag IPs
WCL
IPs
TLR4Flag
SLAMF1
YFP
TRAMYFP
WB: GFP
WB: SLAMF1
WB: Flag
60
30
60
100
TRAMYFP
YFP
SLAMF1
TLR4Flag
D
TLR4Flag IPs
WCL
IPs
TLR4Flag
SLAMF1
TRAMYFP
TRIFHA
WB: GFP
WB: SLAMF1
WB: TRIF
WB: Flag
60
60
100
100
TRAMYFP
SLAMF1
TRIFHA
TLR4Flag
E
TLR4Flag IPs
WCL
IPs
TLR4Flag
SLAMF1
TRIFHA
TRAMYFP
WB: SLAMF1
WB: TRIF
WB: Flag
60
100
100
SLAMF1
TRIFHA
TLR4Flag

Figure 8

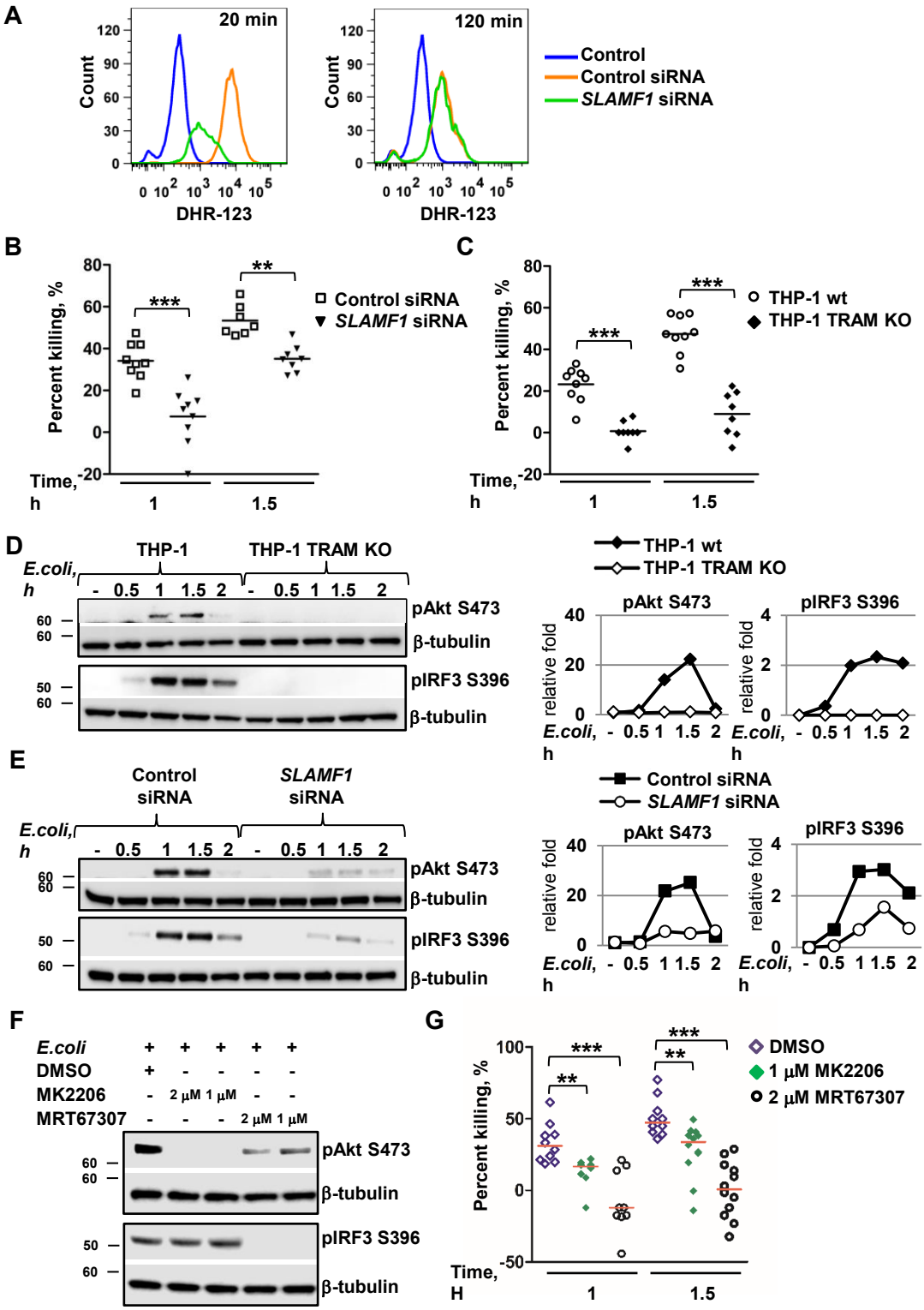
A
20 min
120 min
Count
DHR-123
Control
Control siRNA
SLAMF1 siRNA
B
Percent killing, %
Control siRNA
SLAMF1 siRNA
Time, h
C
THP-1 wt
THP-1 TRAM KO
D
E.coli, h
THP-1
THP-1 TRAM KO
pAkt S473
β-tubulin
pIRF3 S396
relative fold
E
Control siRNA
SLAMF1 siRNA
F
E.coli
DMSO
MK2206
MRT67307
2 μM 1 μM
G
DMSO
1 μM MK2206
2 μM MRT67307

Figure 9

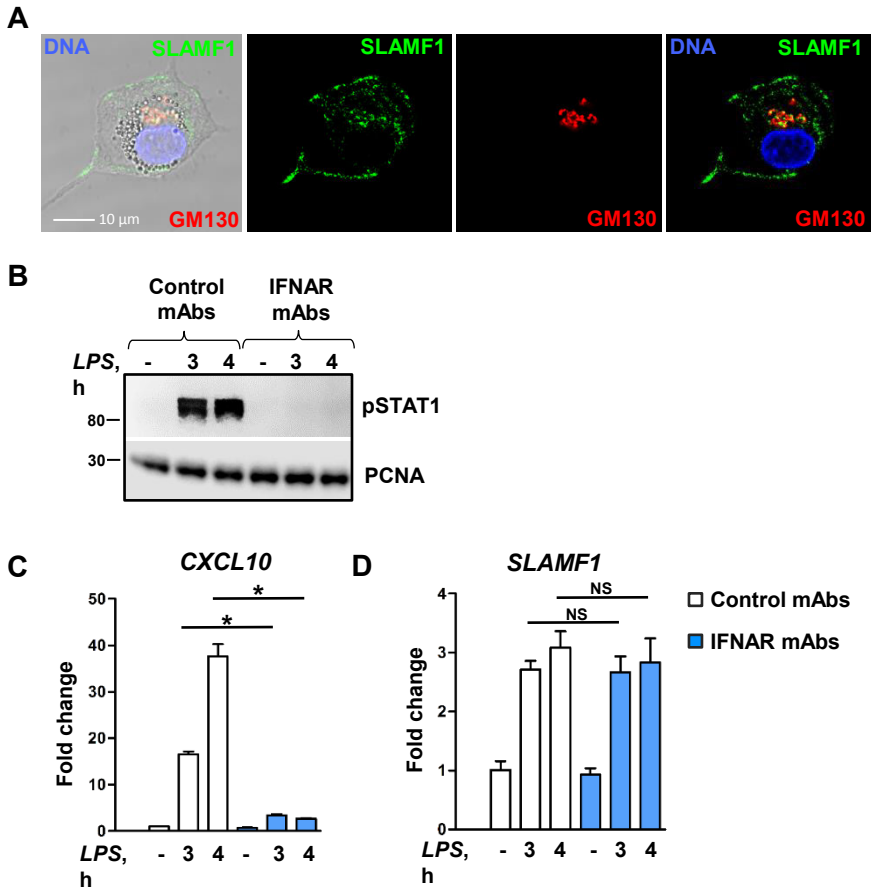

Figure S1. **LPS treatment induces SLAMF1 expression in human cells resulting in its surface localization, and the increase in SLAMF1 expression is not dependent on signaling from the IFNα/β receptor.** (A) SLAMF1 staining in human monocytes after 6 hrs of LPS stimulation. Middle Z-stack of confocal images of a representative cell stained by anti-SLAMF1, anti-GM130 (Golgi marker) antibodies and Hoechst (nuclear staining). Scale bar 10 µm. (B-C) Cells were pre-incubated for 30 min with control mAbs (MOPC-21) or IFN α/β receptor chain 2 (IFNAR) mAbs before addition of LPS for 3 and 4 hrs. Lysates were used for simultaneous isolation of RNA and protein. (B) Proteins analyzed by Western blot analysis for pSTAT1 (Y701) levels, and PCNA Western blot was used for loading control. (C) qPCR data of *SLAMF1* and *CXCL10* mRNA expression from the same experiment as in (B). Western blot results are representative for one independent experiment out of 3. Error bars (C, D) represent mean ± SD for data from three independent experiments, statistical significance evaluated by two-tailed *t*-test, **p* < 0.001. Non-significant differences are marked by NS.

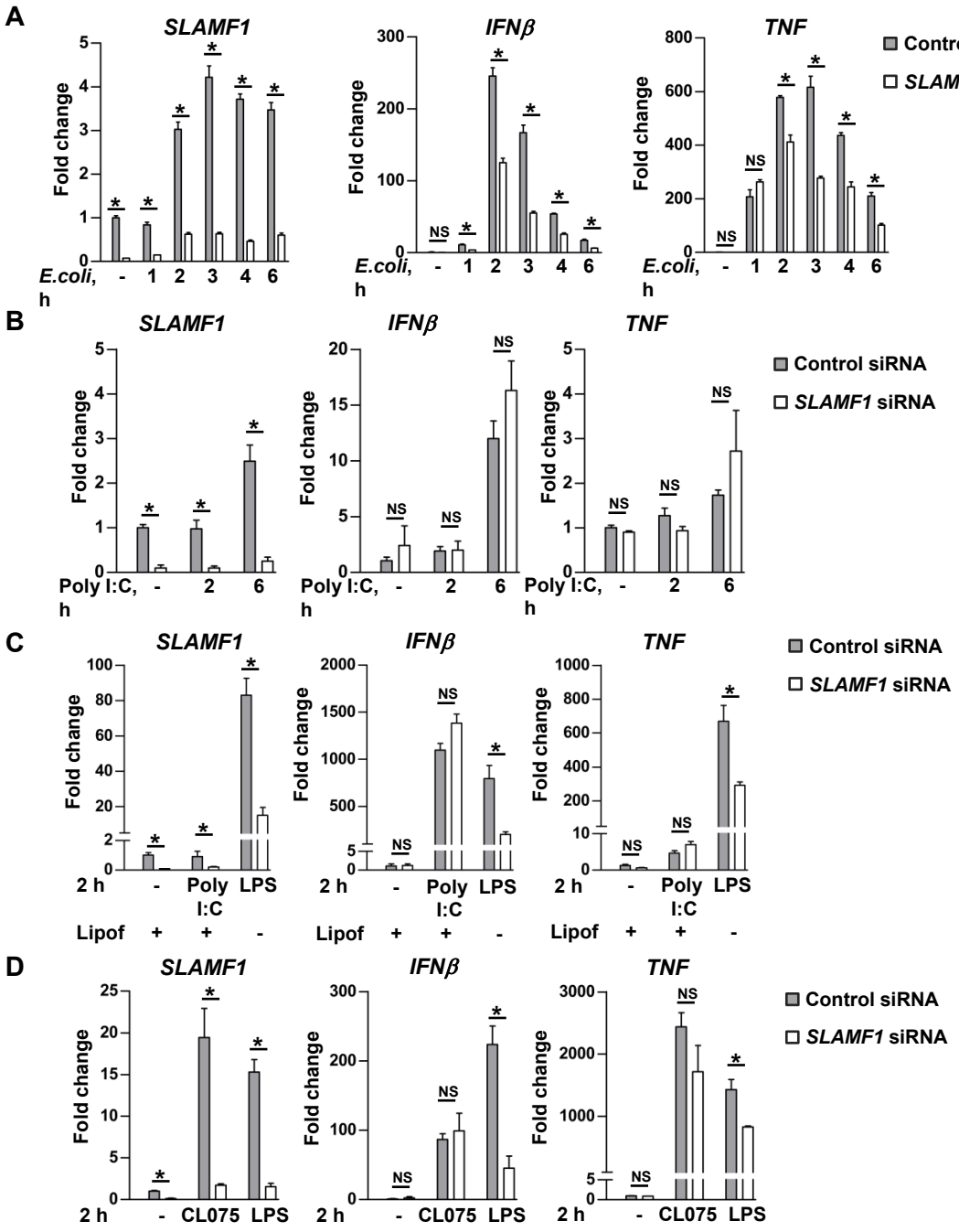

Figure S2. SLAMF1 is involved in regulation of TLR4- (*E.coli*- or LPS-) mediated, but not TLR3-, TLR8- or RIG-1/MDA-5-mediated *IFNβ* or *TNF* mRNA expression. (A) qPCR data of *SLAMF1*, *IFNβ* and *TNF* mRNA expression for THP-1 cells co-cultured with *E.coli* particles for indicated time points, representative of 3 independent experiments. (B-D) Human macrophages silenced by control or SLAMF1 siRNA, and treated with poly I:C (20 μg/ml) for 2 h and 6 h; transfected Poly I:C using Lipofectamin 3000 (Lipof) or LPS (100 ng/ml) for 2 h (C); CL075 (1 μg/ml) or LPS for 2 h (D). Results are representative for three donors (B-D). Error bars show mean ± SD for biological replicates, statistical significance evaluated by two-tailed *t*-test, **p* < 0.01. Non-significant differences are marked by NS.

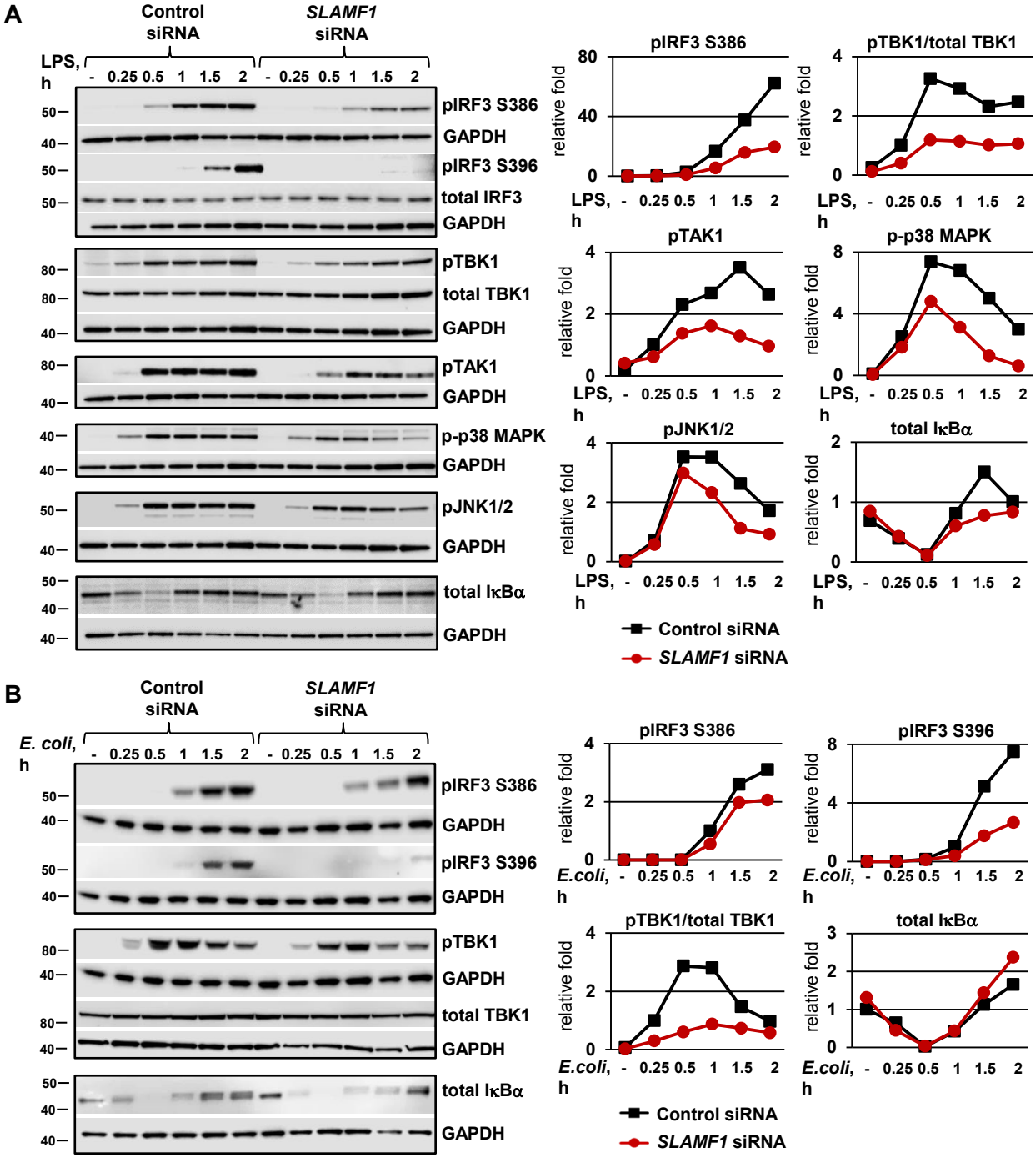

Figure S3. Knockdown of SLAMF1 in THP-1 cells impairs TLR4-mediated phosphorylation of TBK1, IRF3 and TAK1 in response to UP LPS or *E. coli* particles. (A,B) Western blot analysis of lysates from THP-1 cells (representative experiment) treated with control oligo or *SLAMF1*-specific siRNA oligo, and stimulated by UP LPS (A) or *E.coli* particles (B). Graphs (right panels) show quantifications of protein levels relative to GAPDH levels if not stated otherwise on the title. Quantification performed using Odyssey software. Five independent experiments were performed for each treatment condition with almost identical results.

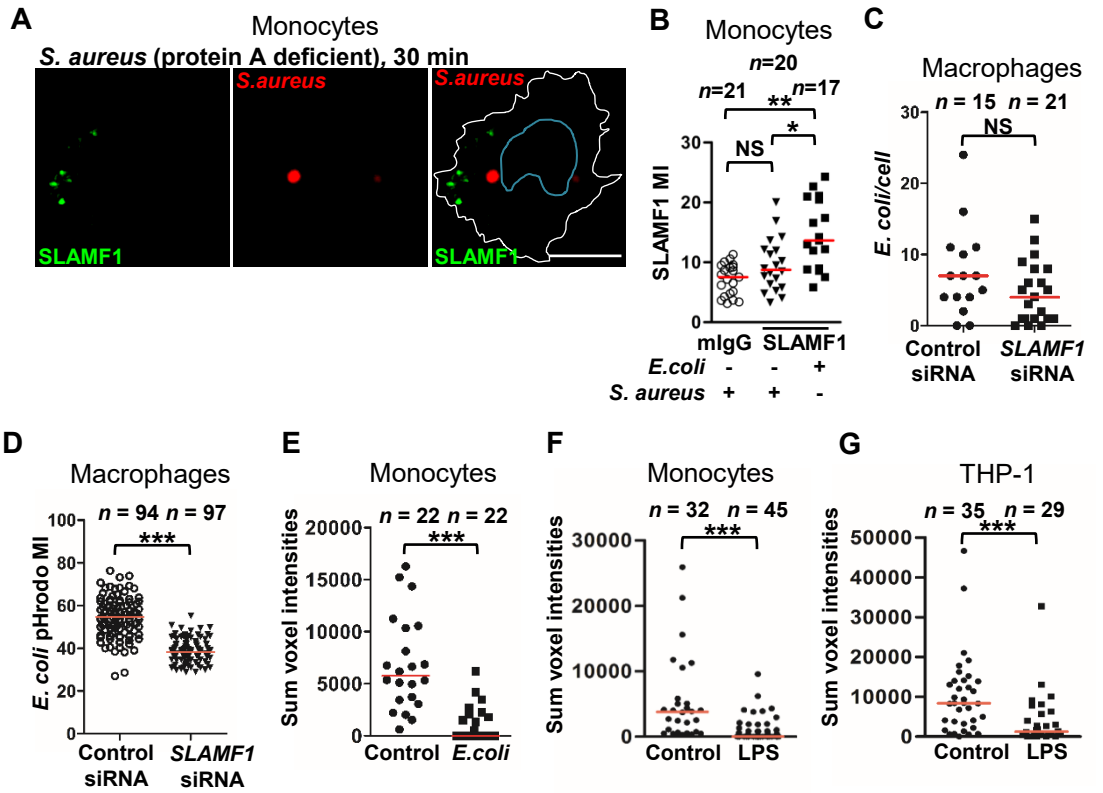

Figure S4. SLAMF1 re-localizes from ERC to early and late *E. coli* phagosomes, but not *S.aureus* phogosomes, and is required for *E. coli* phagosomes acidification in human cells. (A,B) Human monocytes incubated for 30 min ("pulse-chase": 15 min + 15 min) with *S. aureus* and *E. coli* pHrodo particles, fixed and stained for SLAMF1 with representative image for *S. aureus* treated cells (A). Scale bar represent 10 μm. Quantification of SLAMF1 MI around *S. aureus* and *E.coli* phagosomes using ImageJ/Fiji software (B). Numbers of *E.coli* particles uptake per cell (C) and MIs for *E.coli* pHrodo particles (D) in macrophages silenced by control or *SLAMF1* siRNA, co-incubated with particles for 30 min. (E-G) Cells were treated by AF488 *E.coli* particles (E) for 30 min or UP LPS (F,G) for 1 h, followed by immunostaining for GM130 and SLAMF1, and z-stack imaging on confocal microscope. Sum of voxel intensities for SLAMF1 staining inside individual GM130 "rings" was quantified using ImageJ/Fiji software. Data representative of at least three independent experiments. Statistical analysis (B-G) performed using Mann-Whitney test. Lines in the plots represent median, n = number of observations, * $p < 0.01$, ** $p < 0.001$, *** $p < 0.0001$, NS – not significant.

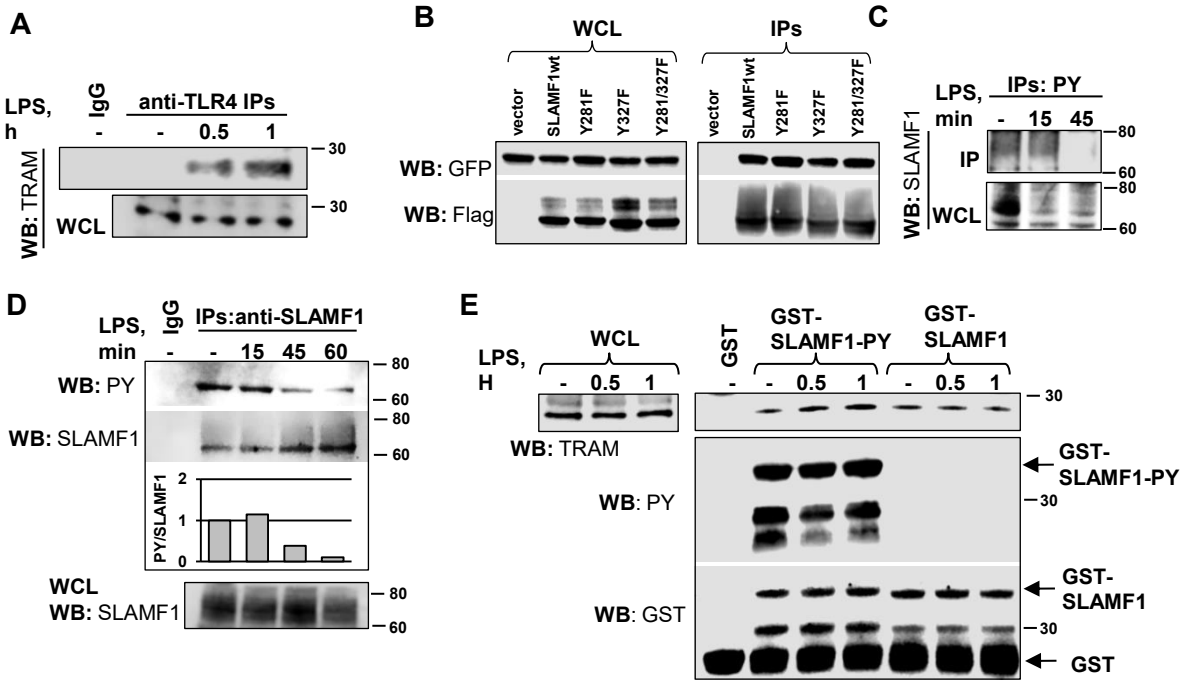

Figure S5. SLAMF1 interaction with TRAM is independent from SLAMF1 tyrosine phosphorylation. (A) TRAM band of expected size was detected after LPS stimulation of macrophages using specific anti-TRAM antibodies in endogenous TLR4 IPs by anti-TLR4 antibodies. (B) Co-precipitations of SLAMF1^{Flag} with point mutations Y281F, Y327F and Y281/327F with TRAM^{YFP}. C Endogenous IPs with anti-phosphotyrosine (PY) biotinylated Abs, followed by precipitation with streptavidin beads and anti-SLAMF1 Western blot analysis. (D) Anti-SLAMF1 IPs, followed by anti-PY and anti-SLAMF1 Western blotting. Anti-IgG control IP was performed from the same amount of lysate of non-stimulated cells (no LPS). Graph represent relative numbers for PY bands density values obtained in Odyssey software and normalized to total SLAMF1 levels in IPs. (E) GST-pull down assays from lysates of macrophages stimulated by LPS at different time points, followed by Western blot analysis for TRAM. Anti-PY Western blot was performed to control tyrosine phosphorylation of GST-SLAMF1-PY recombinant protein, anti-GST Western blot was performed for loading control of fusion proteins. Endogenous IPs and GST-pull down assays were performed from lysates of primary human macrophages, differentiated for 10 days. Data representative of at least three independent experiments.

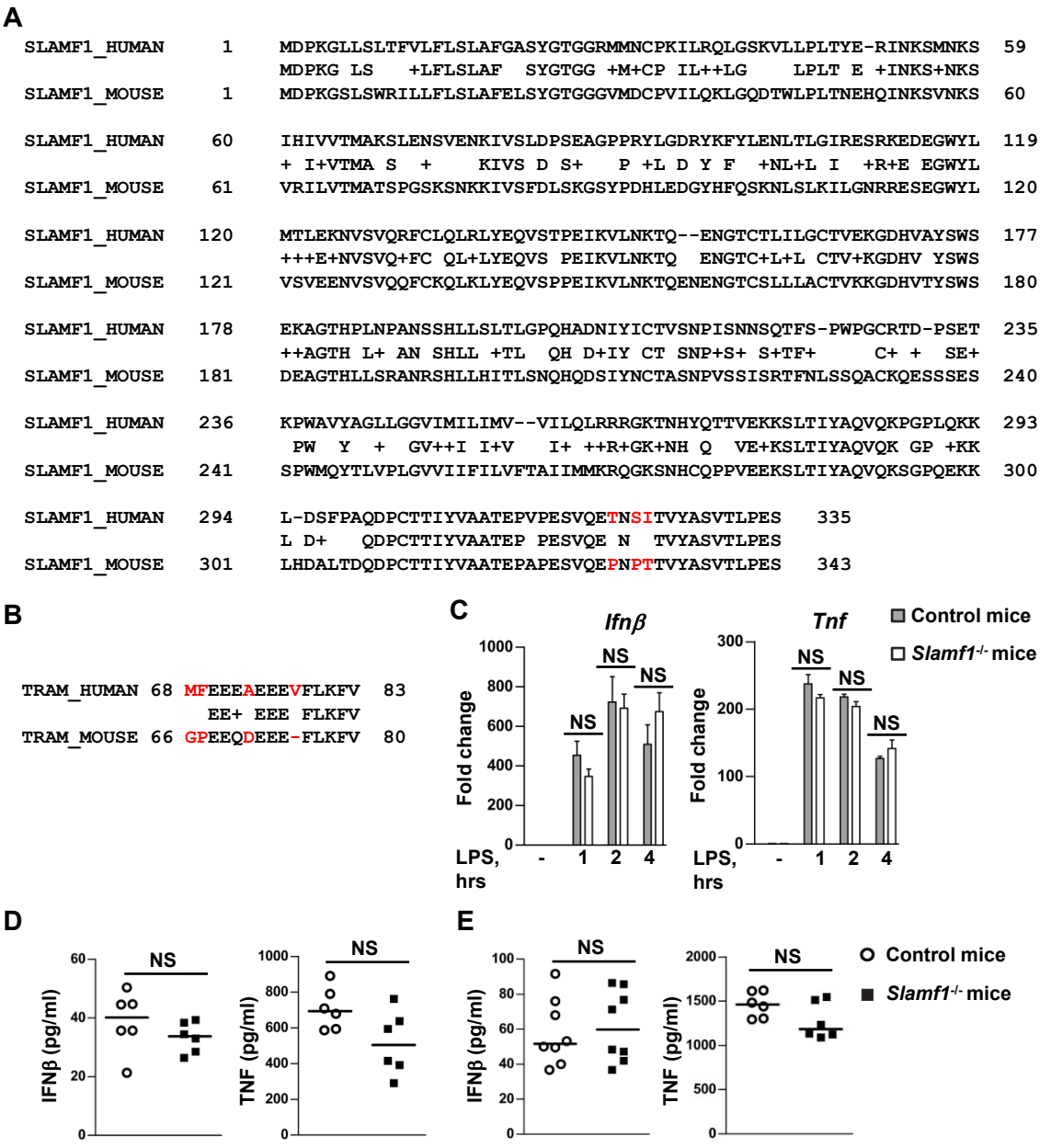

Figure S6. TLR4-mediated *IFNβ* and *TNF* mRNA expression and cytokines' secretion was not altered in *Slamf1*$^{-/-}$ BMDMs. Full sequence alignment of human and murine SLAMF1 proteins (A) and partial alignment of human and murine TRAM proteins in SLAMF1-interacting domain (B); amino acids different in murine and human proteins within SLAMF1ct-TRAM interaction domains are marked by red. (C) *Ifnβ* and *Tnf* mRNA levels by Q-PCR in control and *Slamf1*$^{-/-}$ BMDMs stimulated by UP LPS (100 ng/ml). Error bars represent mean ± SD for combined data from 6 independent experiments, two-tailed *t*-test applied to evaluate statistical significance. (D,E) Quantification of IFNβ and TNF secretion levels in control and *Slamf1*$^{-/-}$ BMDMs stimulated by UP LPS (D) or *E.coli* particles (E) for 6 h, accessed by ELISA. BMDMs isolated from 6 mice both for control and *Slamf1*$^{-/-}$ mice. One dot on graph represents median value of three independent experiments for BMDMS from each mice. Statistical analysis performed using Mann-Whitney test, NS - no significant difference.

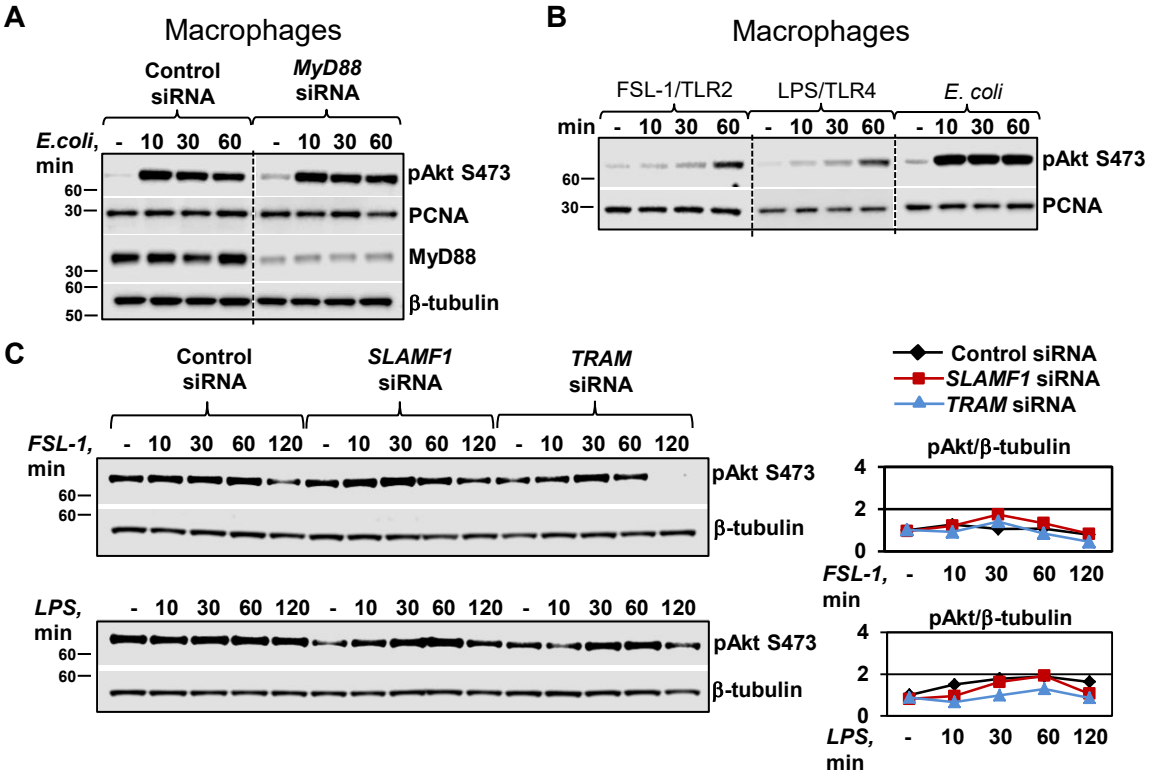

Figure S7. ***E. coli*-mediated Akt phosphorylation in macrophages is not dependent on MyD88 expression, and TLR2- and TLR4-induced phosphorylation of Akt is weak and not much dependent on *SLAMF1* or *TRAM* expression.** (A) pAkt (S473) levels in human macrophages silenced by control siRNA or *MyD88* siRNA. *MyD88* silencing was assessed by anti-MyD88 Western blot. Images in (A) show different parts of the same membranes. Western blot analysis of pAkt in lysates from primary macrophages (B) and THP-1 cells (C) stimulated by FSL-1 (20 ng/ml), K12 LPS (100 ng/ml) or *E. coli* particles (20/cell) (B) for various time points. Images in panel (B) show different parts of the same membranes. THP-1 cells were pretreated with control, *SLAMF1* or *TRAM* specific siRNA prior to stimulation (B). PCNA (A, B) or β-tubulin (A-C) were used as loading controls. Quantification of pAkt (S473) levels (C) was performed in Odyssey software and correlated to basal levels of pAkt and loading controls (graphs on the right).